3D Reconstruction of Helical Specimens

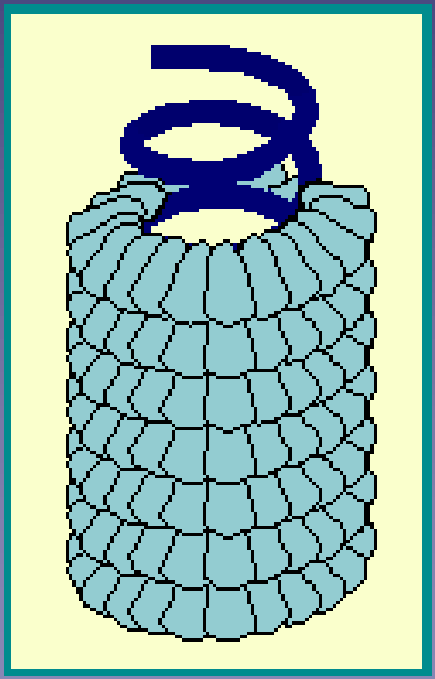

Hernando Sosa
Albert Einstein College of Medicine

Many Biological Specimens have helical symmetry

-DNA
-α-Helix

-Viruses (TMV)
-Actin filaments
-Myosin filaments
-Microtubules
-Bacterial Flagella
-Protein-lipid tubes

Lecture outline

- Helix definition.
- Fourier Transform of a Helix.
- Fourier-Bessel Helical 3D reconstruction
- Real space Helical 3D reconstruction.
- Some examples.

Helical Symmetry

Combining the symmetry operation of **translation and rotation** (screw) produces a **helix**

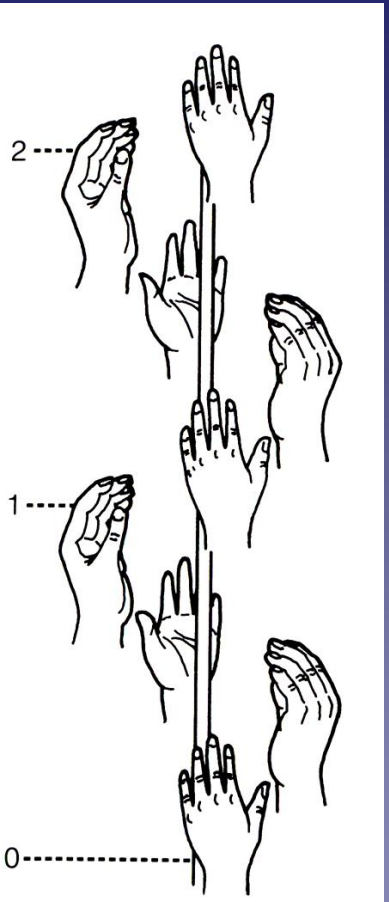

4_1 on left hand

(**b**)

Possible Symmetry operations:

-Screw.

-n-fold rotation about axis.

-2-fold rotation perpendicular to axis.

Parameters of a Helix

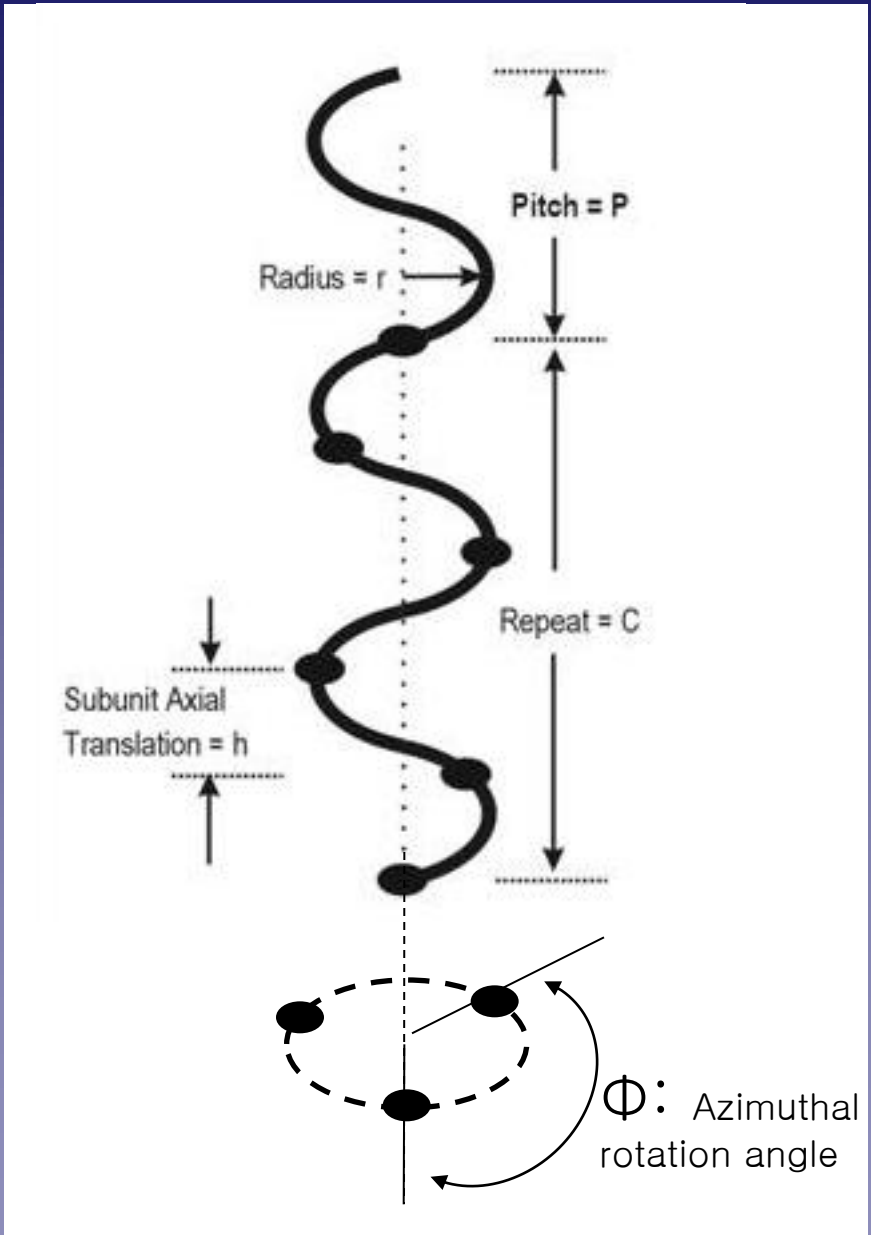

Helices give several orientation views of the asymmetric unit from a single view direction

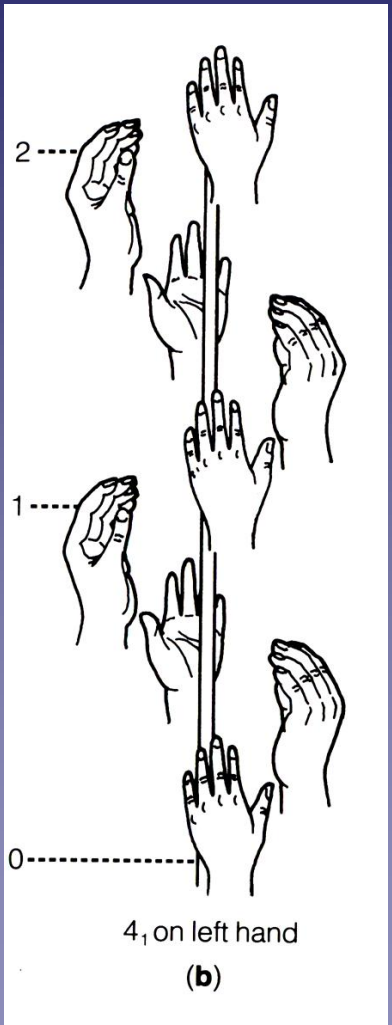

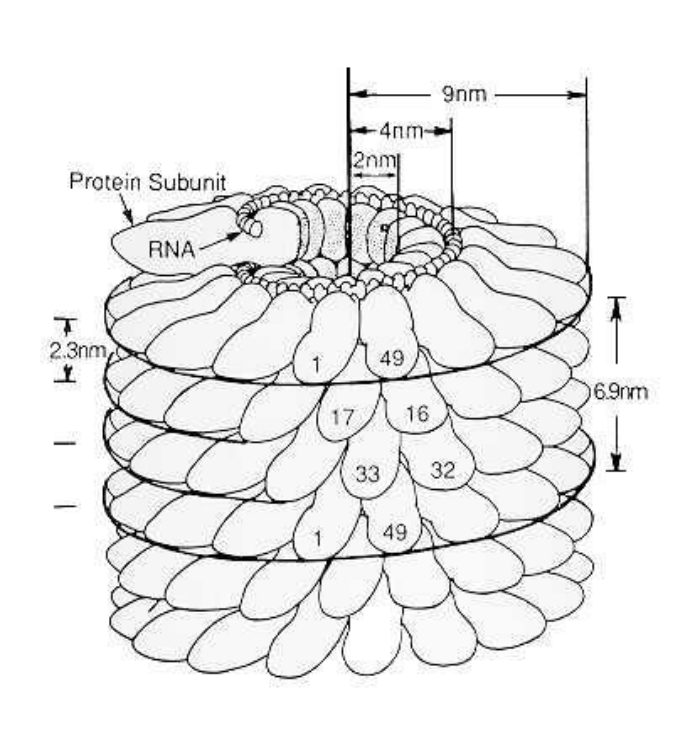

Reconstruction of Three Dimensional Structures from Electron Micrographs

by

D. J. DE ROSIER
A. KLUG

MRC Laboratory of Molecular Biology,
Hills Road, Cambridge

General principles are formulated for the objective reconstruction of a three dimensional object from a set of electron microscope images. These principles are applied to the calculation of a three dimensional density map of the tail of bacteriophage T4.

The standard high resolution electron microscope has a depth of focus of several thousand Ångström, making the image a two dimensional superposition of different levels in the three dimensional structure. The focus cannot be adjusted to different levels within the object, and so three dimensional structures are difficult to analyse. Stereo-electron micrographs do not overcome this difficulty satisfactorily, as will be shown.

Our method starts from the obvious premise that more than one view is generally needed to see an object in three dimensions. We determine first the number of views required for reconstructing an object to a given degree of resolution and find a systematic way of obtaining these views. The electron microscope images corresponding to these different views are then combined mathematically, by a procedure which is both quantitative and free from arbitrary assumptions, to give the three dimensional structure in a tangible and permanent form. The method is most powerful for objects containing symmetrically arranged subunits, for here a single image effectively contains many different views of the structure. The symmetry of such an object can be introduced into the process of reconstruction, allowing the three dimensional structure to be reconstructed from a single view, or a small number of views. In principle, however, the method is applicable to any kind of structure, including individual, unsymmetrical particles, or sections of biological specimens.

Summary of Procedure

Electron micrographs are selected in which the details of the structure show up best, as judged for example in the phage tail described later, by their optical diffraction patterns[1,2]. The optical density in each image is sampled at regular points on a grid by an automatic microdensitometer linked to a computer (established work of U. W. Arndt, B. A. Crowther and J. F. W. Mallett), which converts the image into a set of numbers representing the density at each grid point. These numbers are now transformed by computation into a set of Fourier

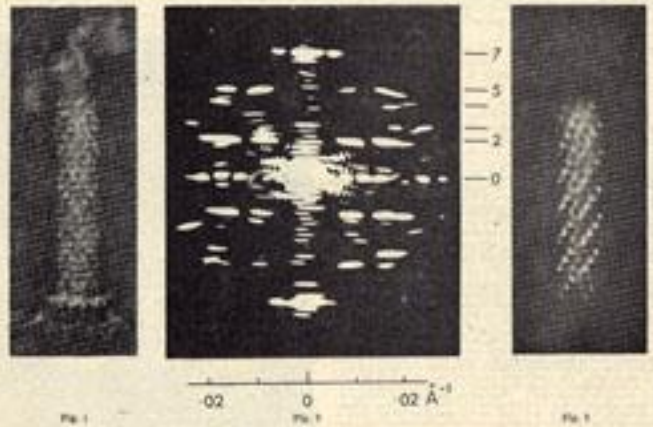

Fig. 1. Electron micrograph of a tail of bacteriophage T4, negatively stained with uranyl formate. (× 100,000.)

Fig. 2. Optical diffraction patterns of the phage tail image in Fig. 1. Moiré patterns show that the order in the micrograph extends to spacings of about 20 Å. The sixth meridional peak on the outside have now gone from the spacing of 50 Å between crests. The layer lines are approximately equally spaced at the orders of an approximate repeat of T = 50 × 360 Å. The lattice reflections take for the diffraction pattern in (a) to (c), the only plausible values of a being those which are multiples of six.

Fig. 3. Optically filtered image of phage tail in Fig. 1, admitting only the diffracted rays corresponding to the far side of the particle. The individual features are two distinct arcs of lattice structure, which correspond to two distinct sets of helical lines running along the cylindrical surface of different diameter, and also correspond to helices of different angles in the particle.

De Rosier & Klug. Nature 217: 130-134 1968

3D reconstruction approaches

2D crystals

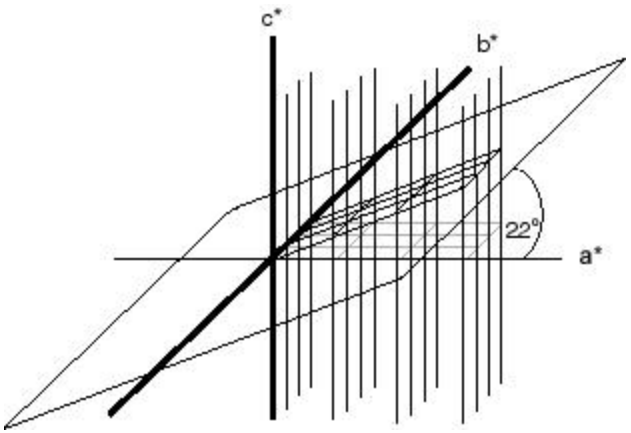

Helical crystals

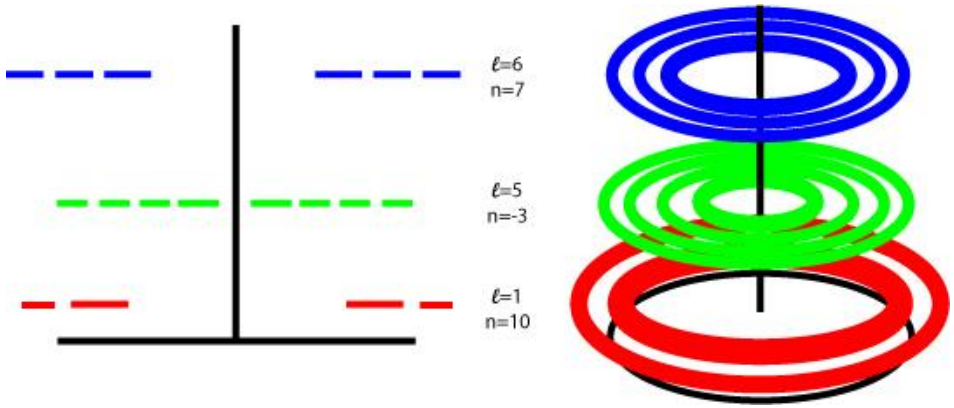

Single particles/viruses

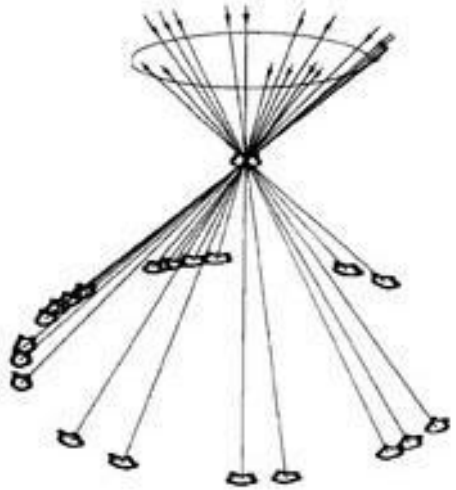

tomography

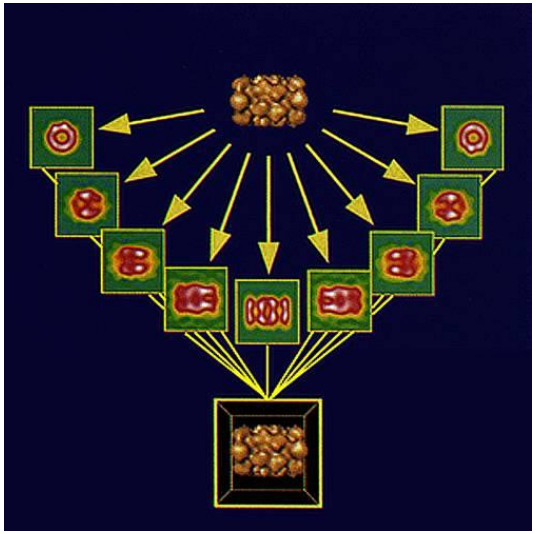

No Missing Cone !

2D crystals

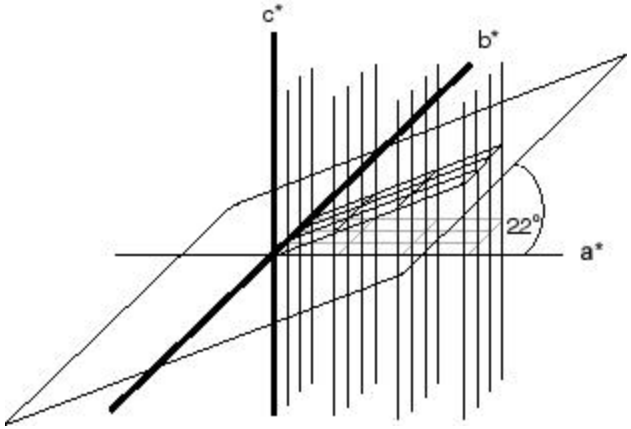

missing cone

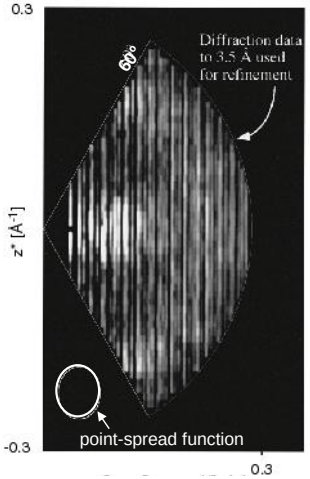

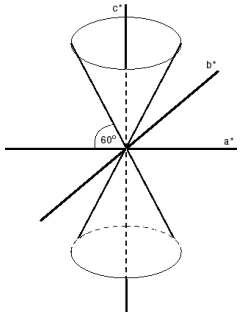

Helical crystals

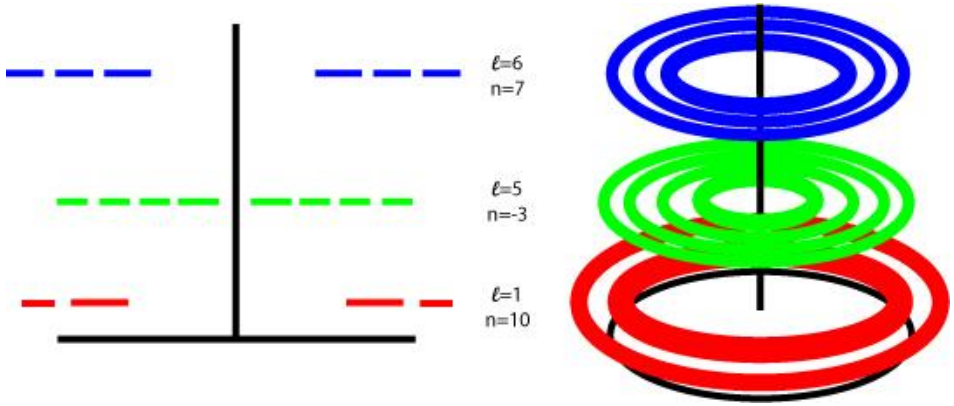

The Helical Latice Radial Projection

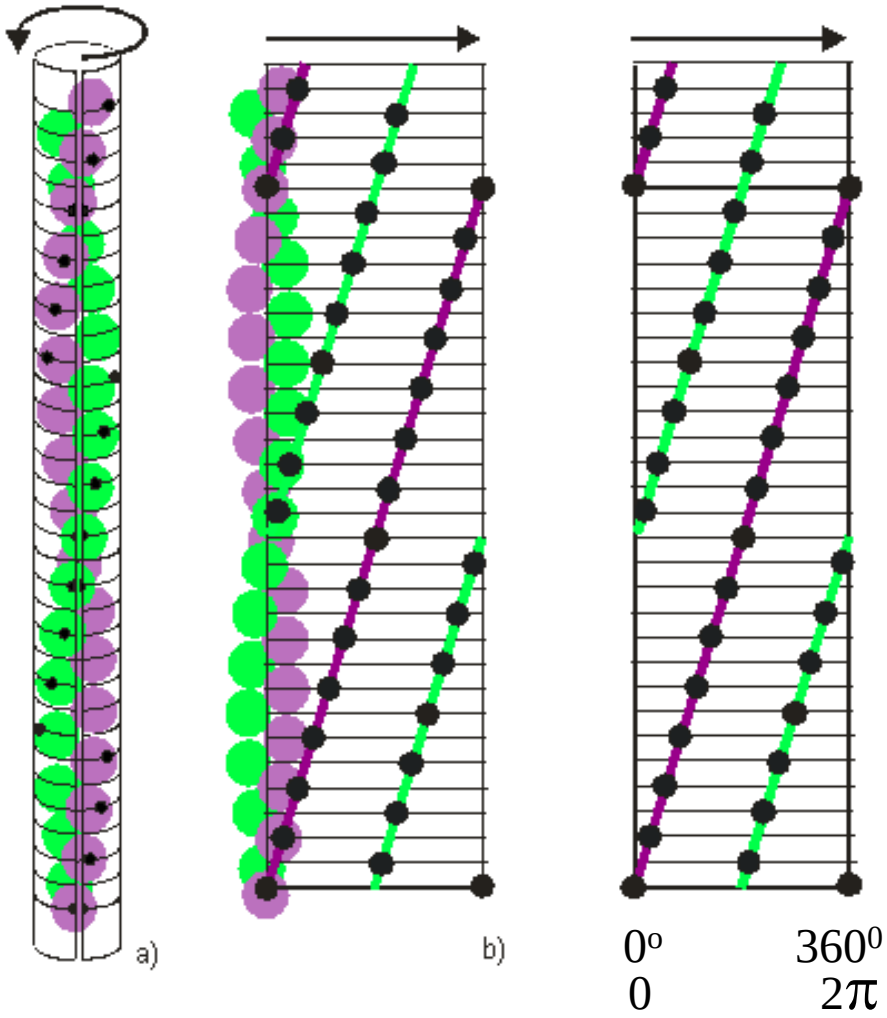

Analogy between 2D lattices and Helical Lattices

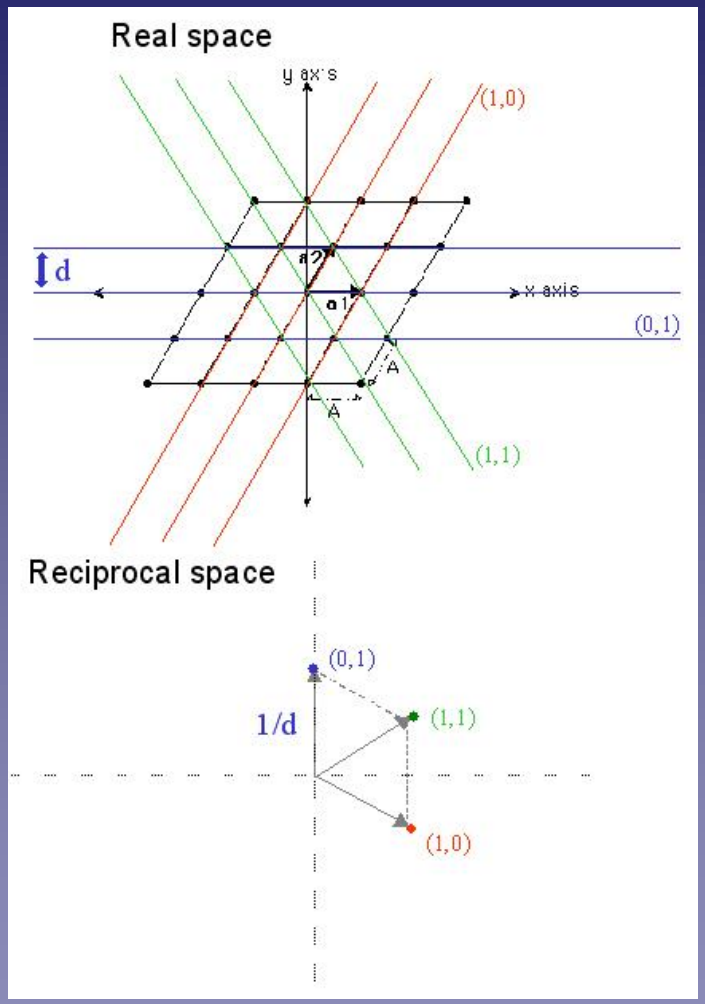

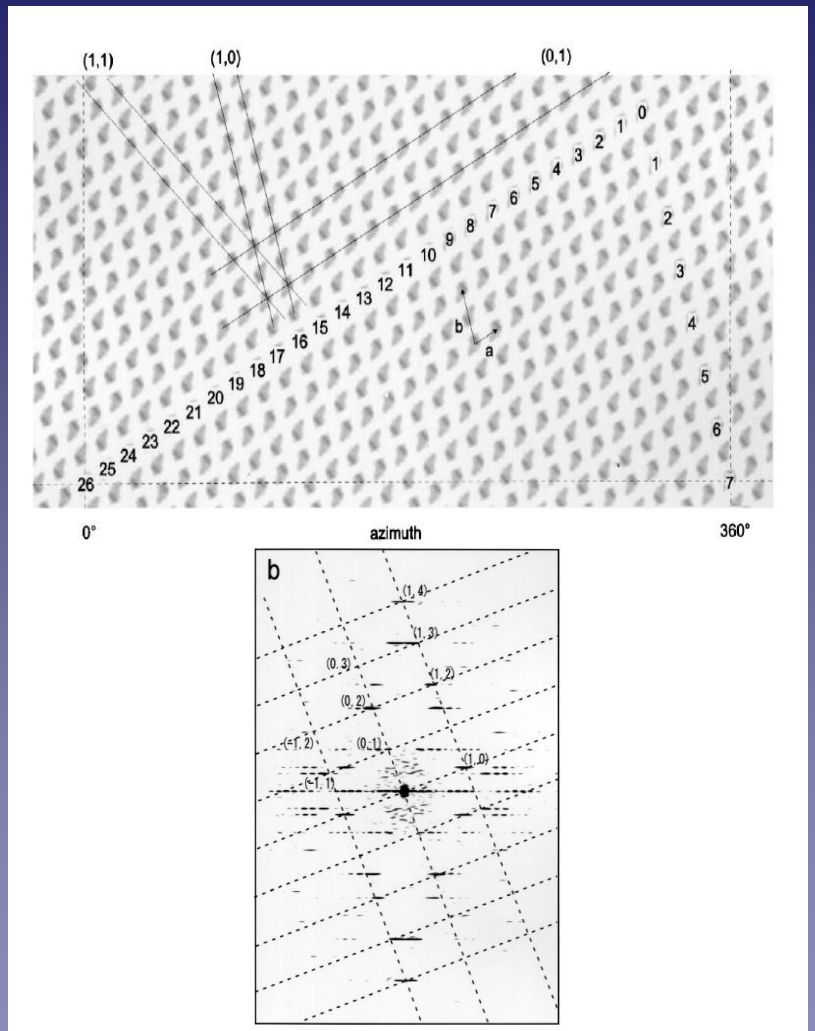

From: Toyoshima (2000) Ultramicroscopy 84: 1-14

Analogy between 2D Fourier synthesis and Fourier-Bessel helical synthesis

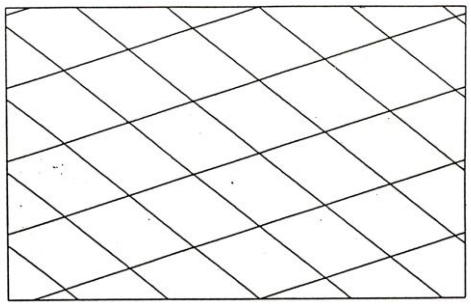

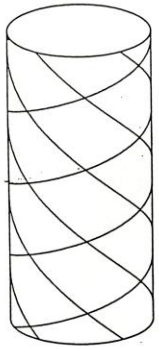

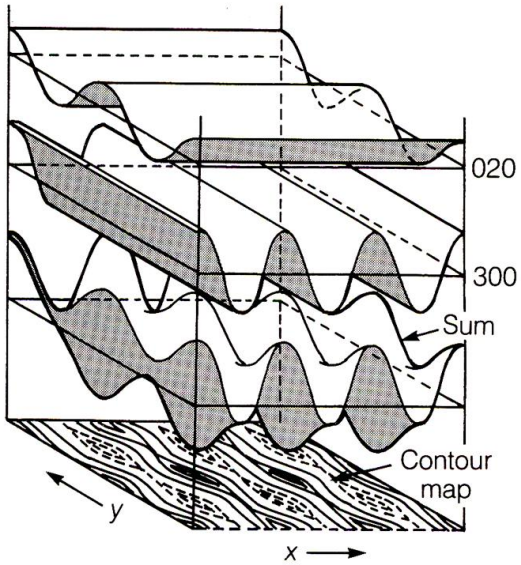

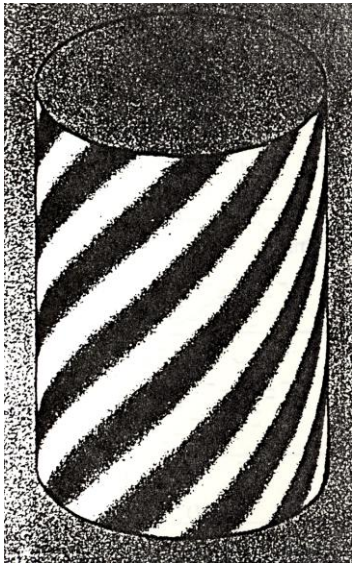

Summation od 2D waves to produce a 2D density map. (From Jeffery 1972)

A helical wave

The Fourier Transform of a Helix

$$T(R, \psi, n/P) = J_n(2\pi Rr) \exp\left[in(\psi + \tfrac{1}{2}\pi)\right]$$

Cochran, Crick & Vand 1952

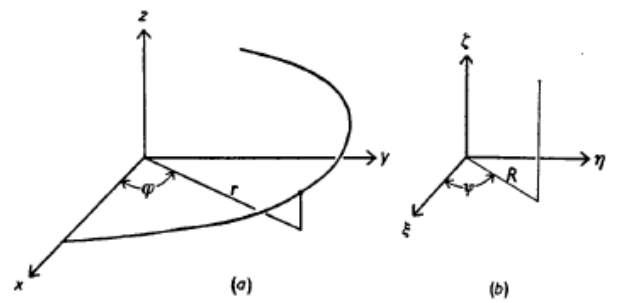

Fig. 1. (*a*) Cartesian (x, y, z) and cylindrical-polar (r, φ, z) co-ordinates of a point on a helix. (*b*) Corresponding coordinates of a point in reciprocal space.

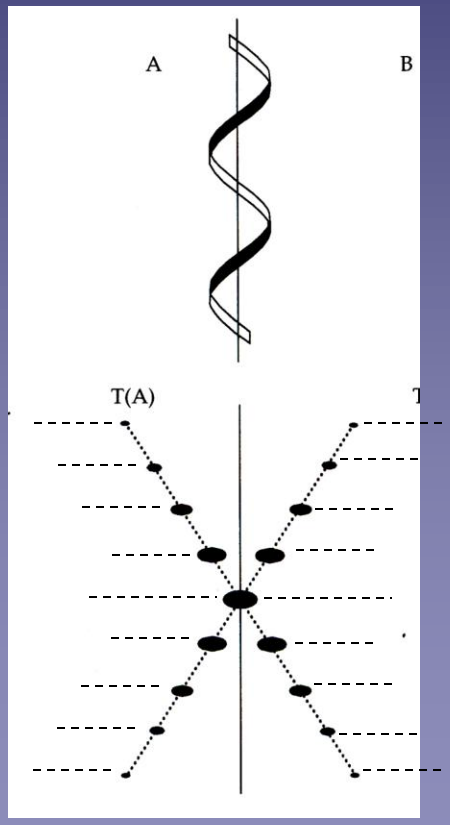

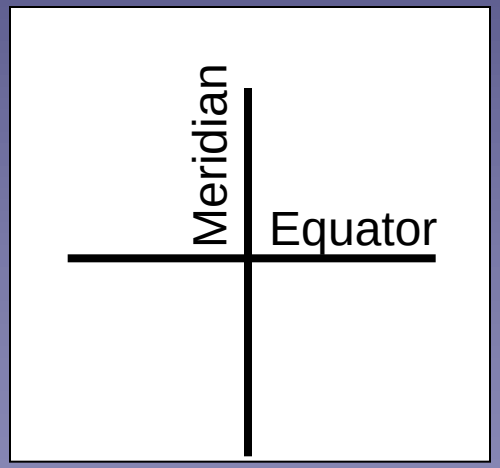

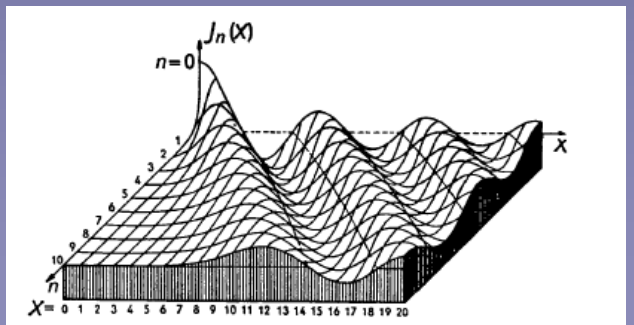

Fig. 2. Illustration of Bessel functions. (Reproduced by kind permission of the publishers from *Tables of Functions* by Jahnke & Emde. New York: Dover Publications.)

The Transform of a discontinuous helix

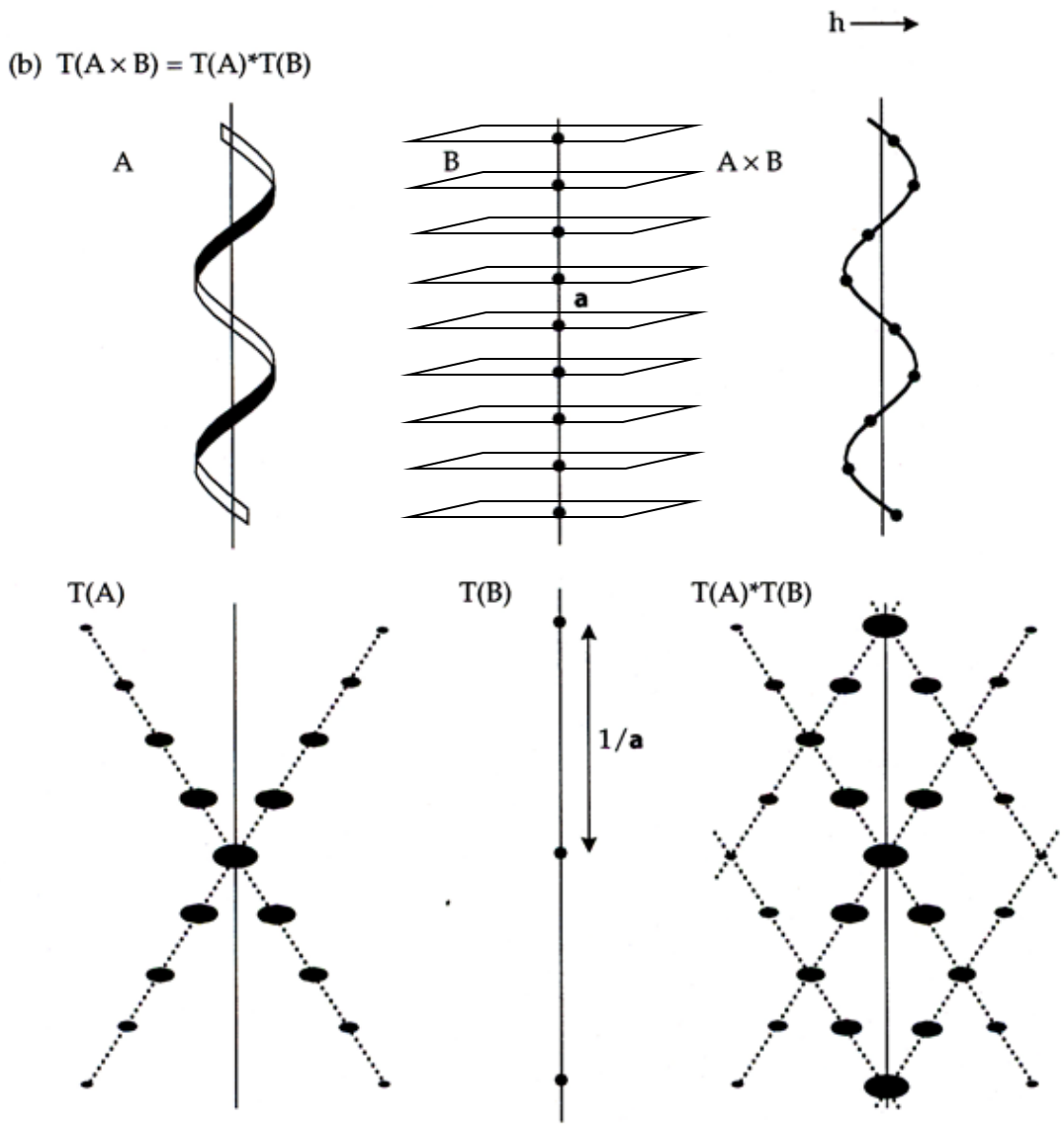

A helix and its corresponding Fourier Transform (Power Spectrum)

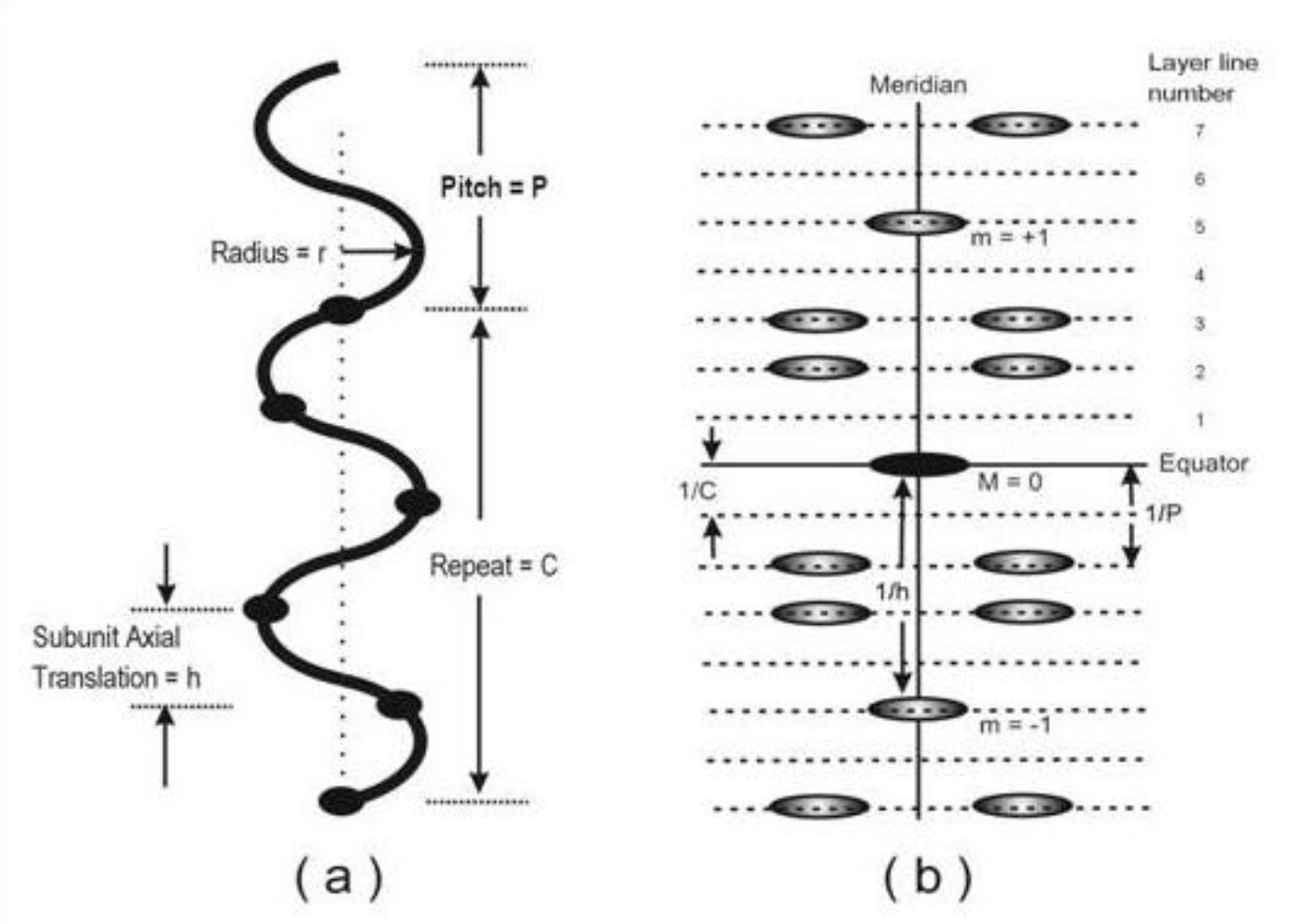

The DNA Structure

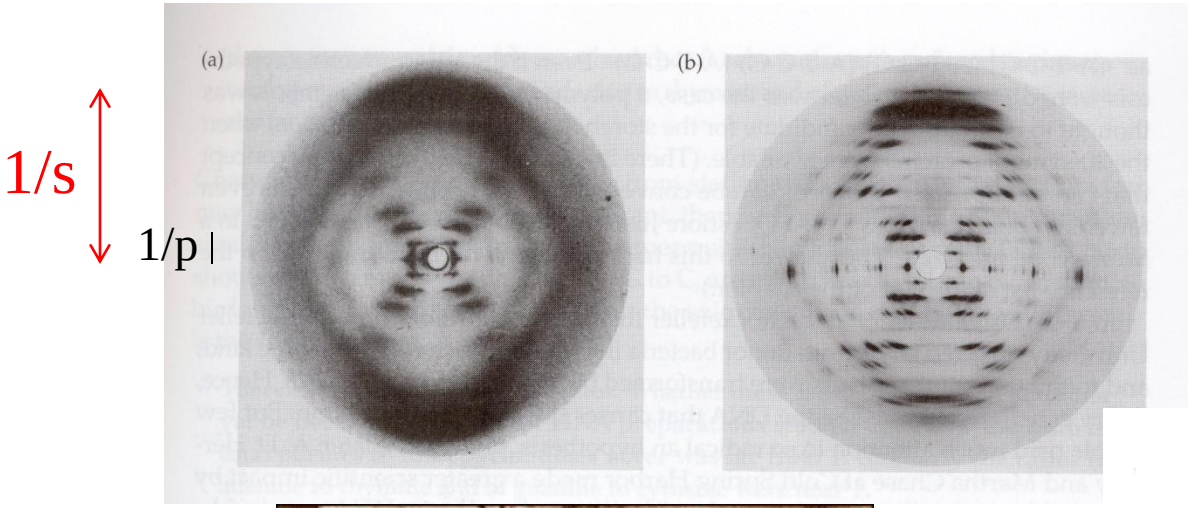

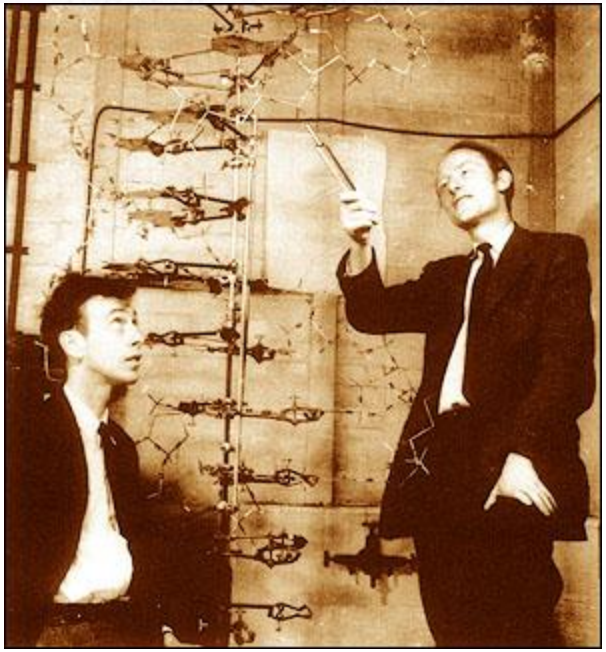

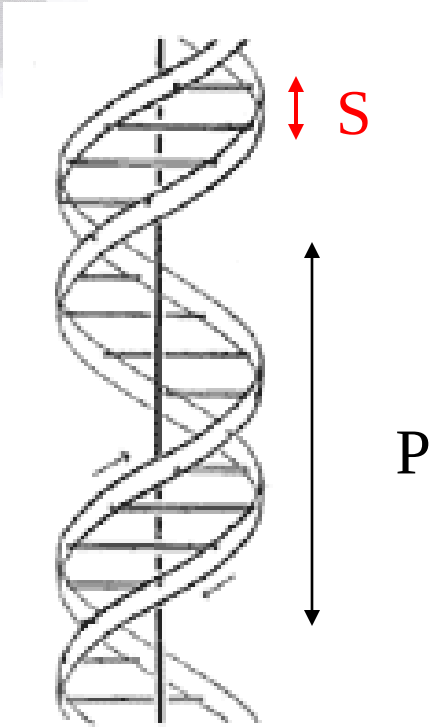

The Fourier Bessel Transform

$$T(R, \psi, n/P) = J_n(2\pi Rr) \exp\left[in(\psi + \tfrac{1}{2}\pi)\right]$$

Cochran, Crick & Vand 1952

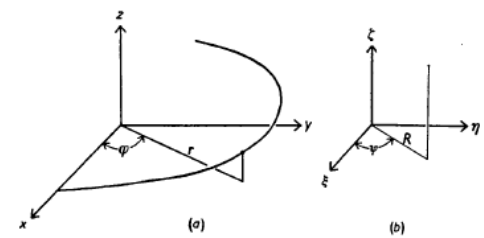

Fig. 1. (a) Cartesian (x, y, z) and cylindrical-polar (r, φ, z) coordinates of a point on a helix. (b) Corresponding coordinates of a point in reciprocal space.

Tranform of group of j atoms at differnt radii

$$G_{n,l}(R) = \sum_j f_j J_n(2\pi R r_j) \exp\left[i\left(-n\varphi_j + \frac{2\pi l z_j}{c}\right)\right].$$

$$F(R, \psi, l/c) = \sum_n G_{n,l}(R) \exp\left[in(\psi + \tfrac{1}{2}\pi)\right],$$

Klug, Crick & Wickoff 1958

Why we can get a 3D structure from a single view?
The real and reciprocal space (Fourier transform) arguments

$$F(R, \Phi, l/c) = \sum_n G_{n,l}(R) \exp\left[in\left(\Phi + \pi/2\right)\right].$$

$$F(R, \Phi, l/c) = \quad G_{n,l}(R) \exp\left[in\left(\Phi + \pi/2\right)\right].$$

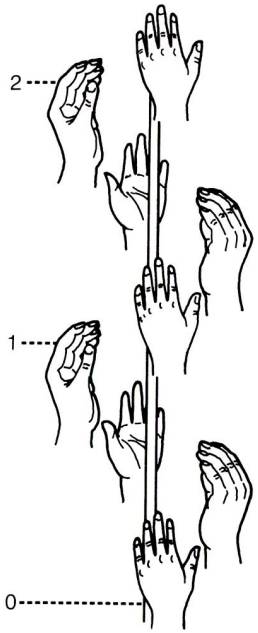

4_1 on left hand

(**b**)

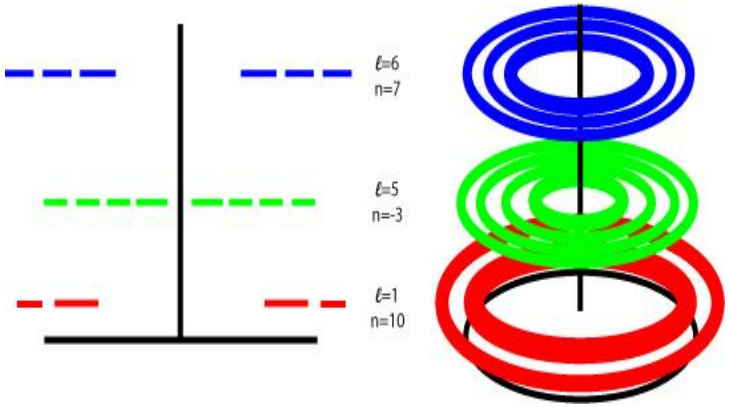

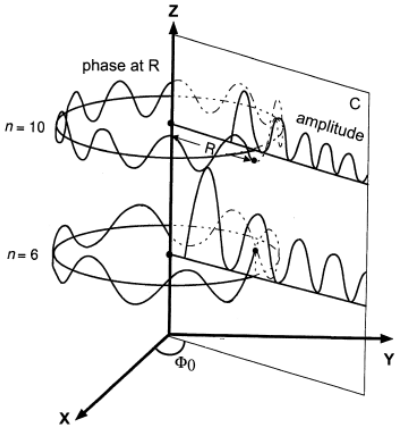

The Selection Rule

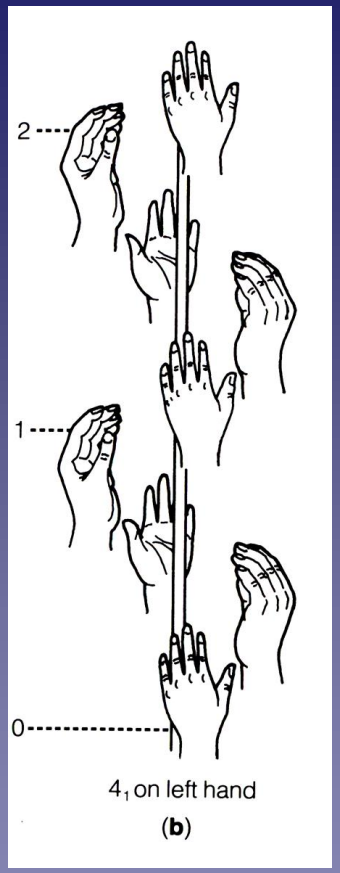

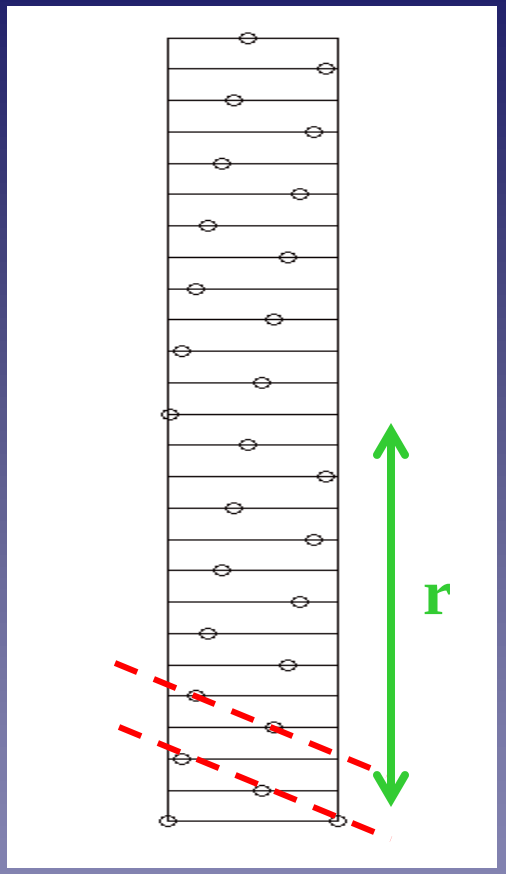

4 units in 1 Turn (RH)

13 units in 6 Turns (LH)

Knupp C, Squire JM, **HELIX: A helical diffraction simulation program**, J Appl Cryst, 2004, Vol: 37, Pages: 832 - 835

http://www.ccp13.ac.uk/software/program/Helix/INDEX.htm

The Selection Rule

$$l = tn + um$$

l **:** Layer line Number.
t **:** Num. of turns/rep.
n**:** Num of Helical starts & bessel order.
u**:** Num. of subunits/rep
m**:** Integer

If ***k***-fold rotational symmetry then:
n must be multiple of ***k***

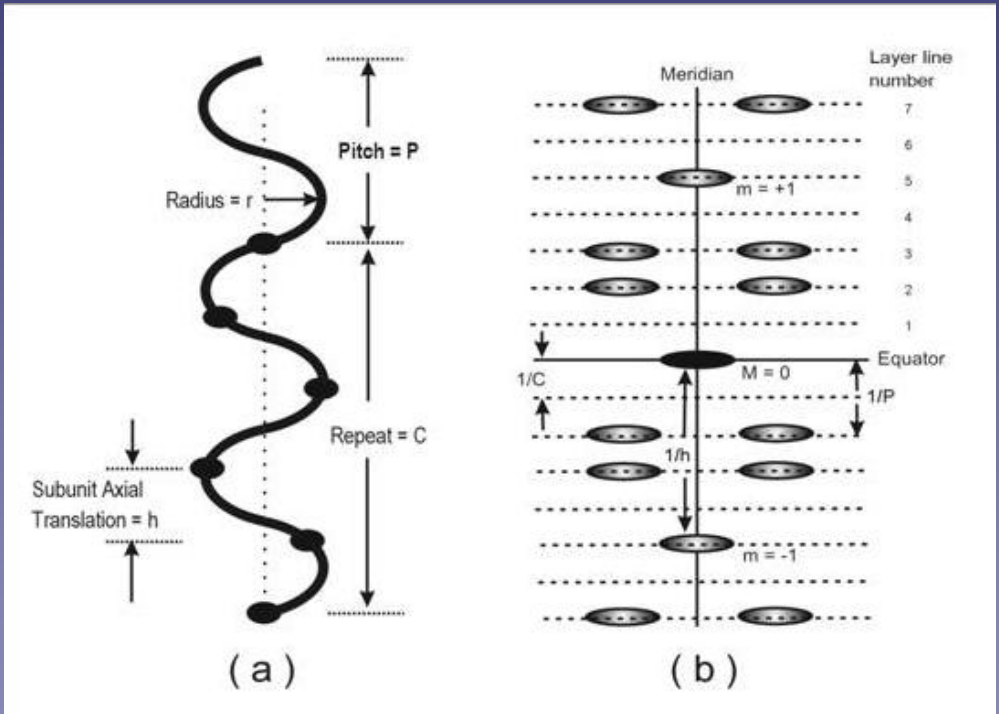

$$Z = n(\Phi/360^0)/h + m/h$$

Z: LL reciprocal spacing
Φ: Azimuthal angle. per subunit
h: rise distance. per subunit

Selection Rule Example

$$l = tn + um$$

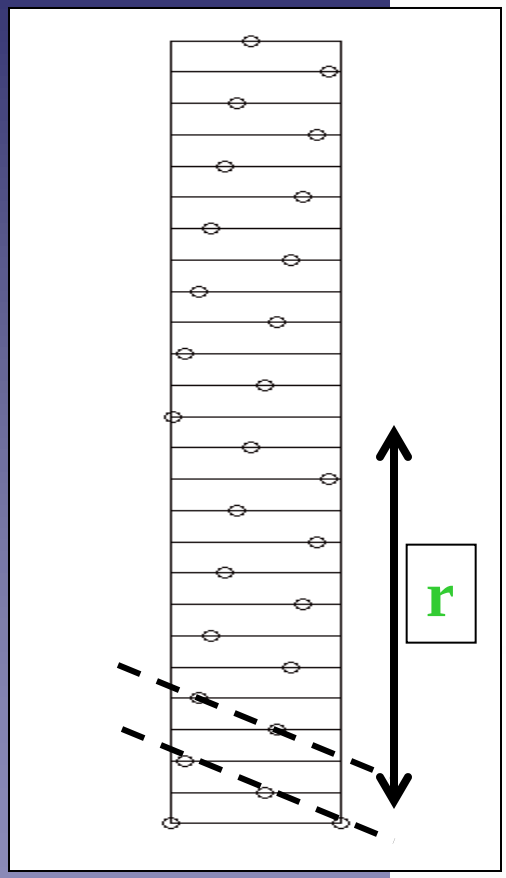

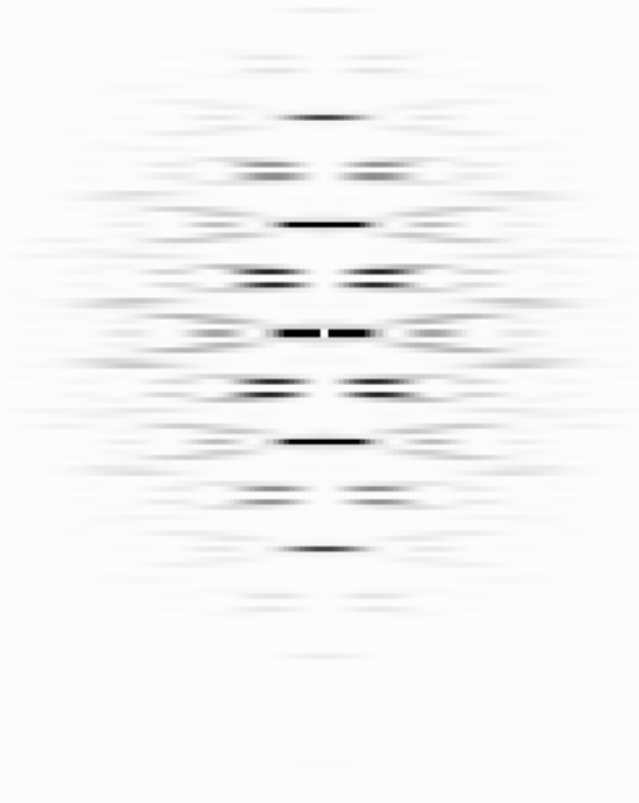

l	n ($\lvert n\rvert <= 10$)
0	0
1	2
2	4, -9
3	6
4	-5, 8
5	-3, 10
6	-1
7	1
8	3, -10
9	5, -8
10	-6, 7
11	-4, 9
12	-2
13	0

$$l = -6n + 13m$$

Finding Helical Symmetry Selection Rule
Indexing the diffraction Pattern

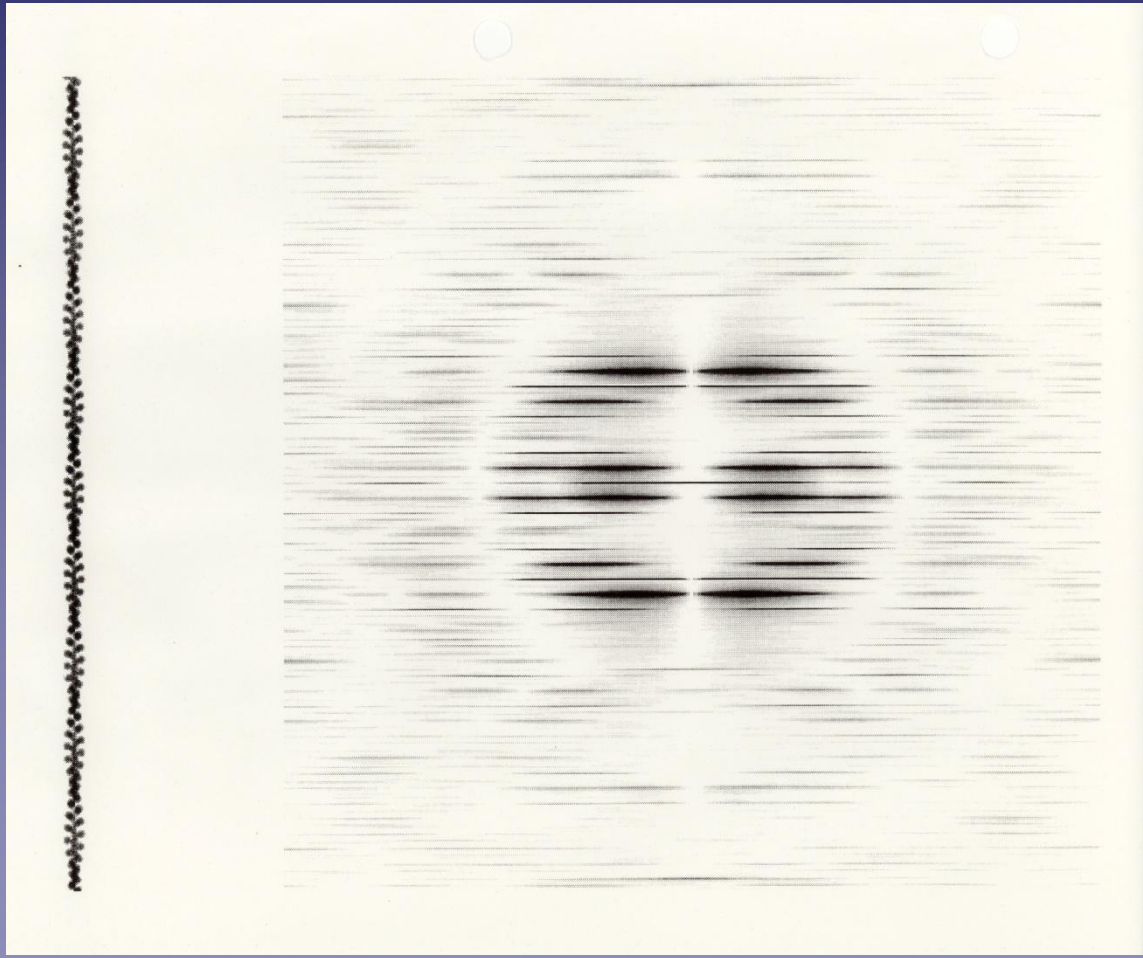

Clues to trace the Reciprocal Helical Lattice:

Approximate value of |n| for each layer line is: $|n|+2 = 2\pi Rr$.
r: Helix radius, R: Reciprocal of layer line peak position to the meridian.

- Determine if n is odd or even by looking at mirror symmetric peaks from the meridian. Even if same phase, Odd if phase diff = 180°.

- Determine hand of helical paths (sign of n). Shadow or tilt specimens.

-The dimension of the unit vectors should be aproximately equal to the inverse of the subunits dimensions. $d=1.34(m)^{1/3}$ (d in Å, m in daltons) (e.g actin dimensions ~ 5 nm)

- Draw n,Z plot.

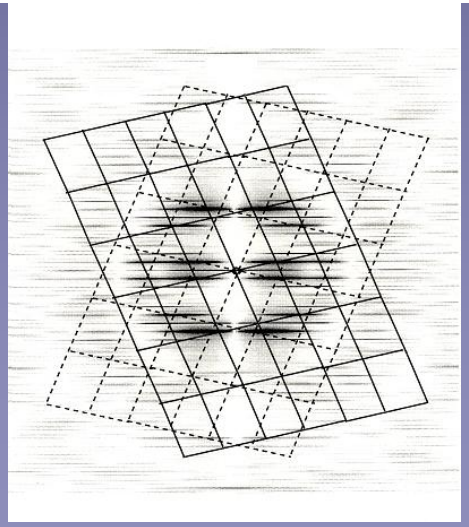

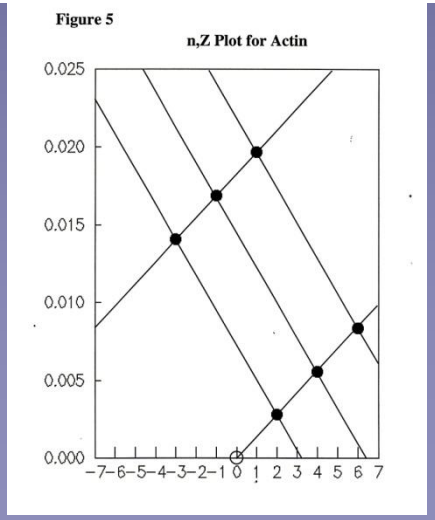

Flattening increases apparent radius of helical tubes

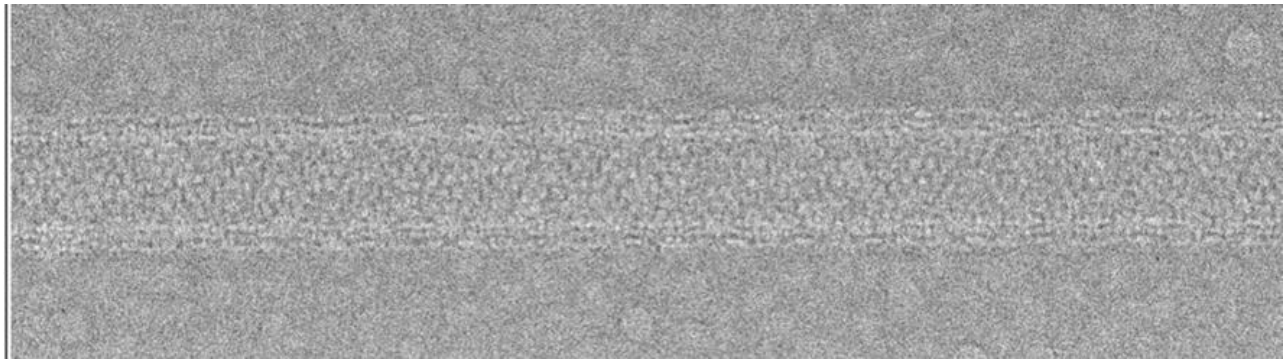

Cryo-em

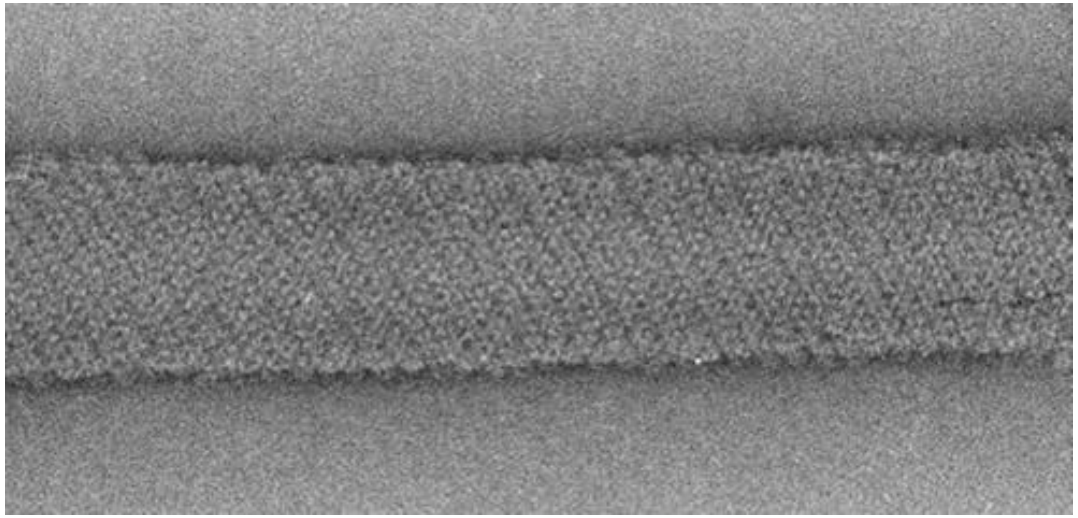

Negative staining

Indexing the diffraction Pattern

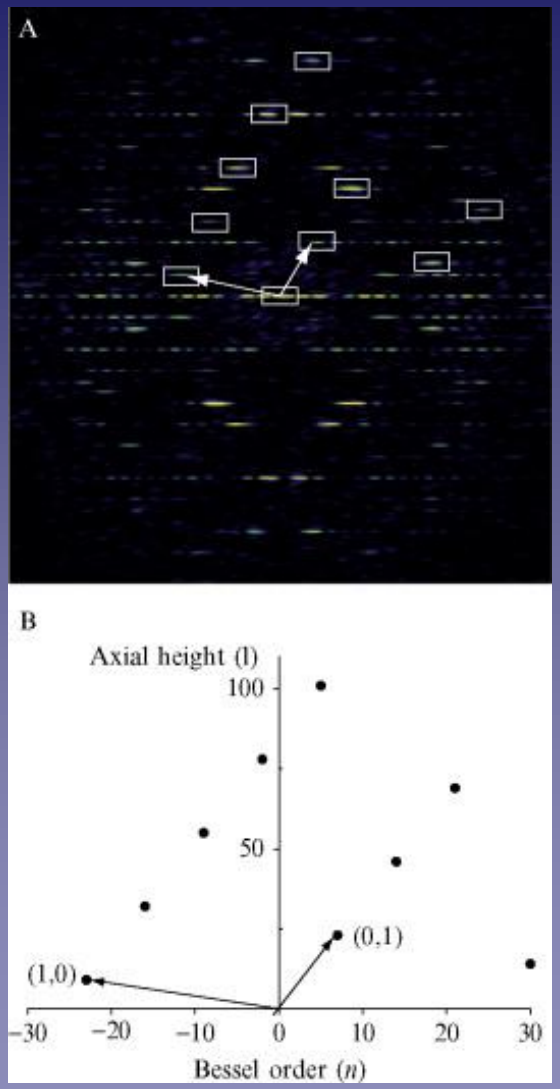

From: Diaz et al., Methodsin Enzymol.482: 131-165 (2010)

The Diffraction Pattern of a Helix Has Reflections From Planes in the Front and Back of the Helix

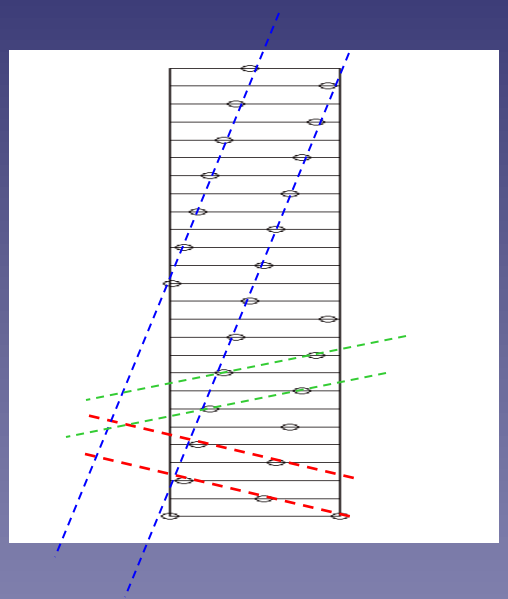

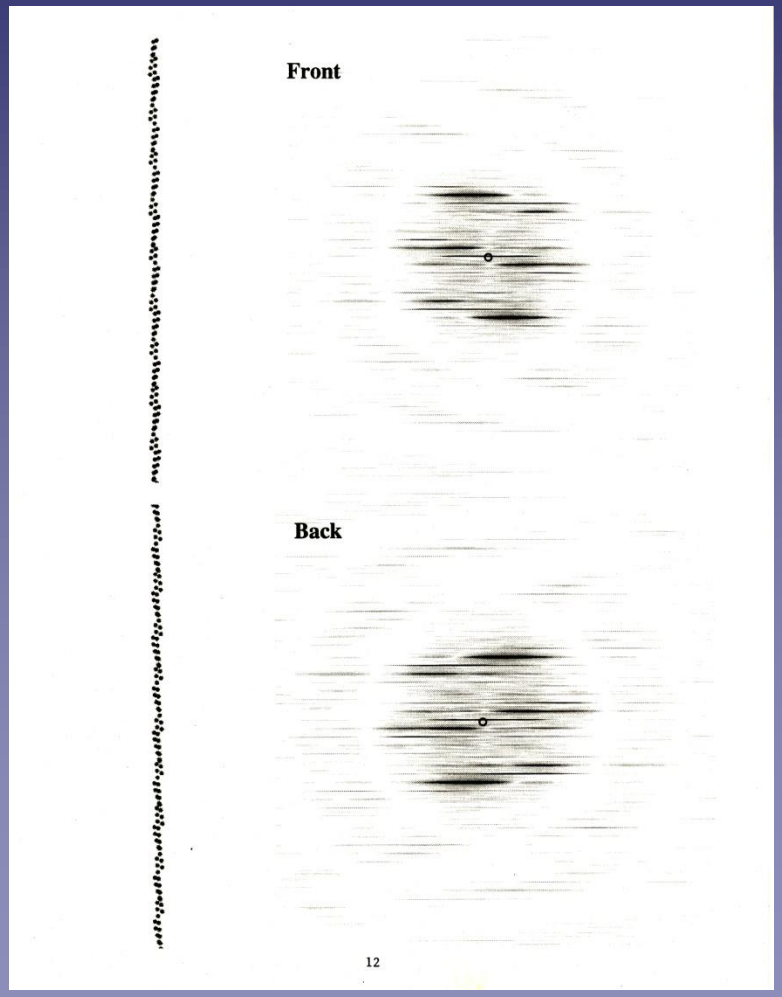

Different from the case of the transfrom of a 2D lattice where reflections from a set of planes form a spot in Fourier space. In the case of a helix the reflections are continuous Bessel function along “layer” lines.

Drawing the Reciprocal Lattice

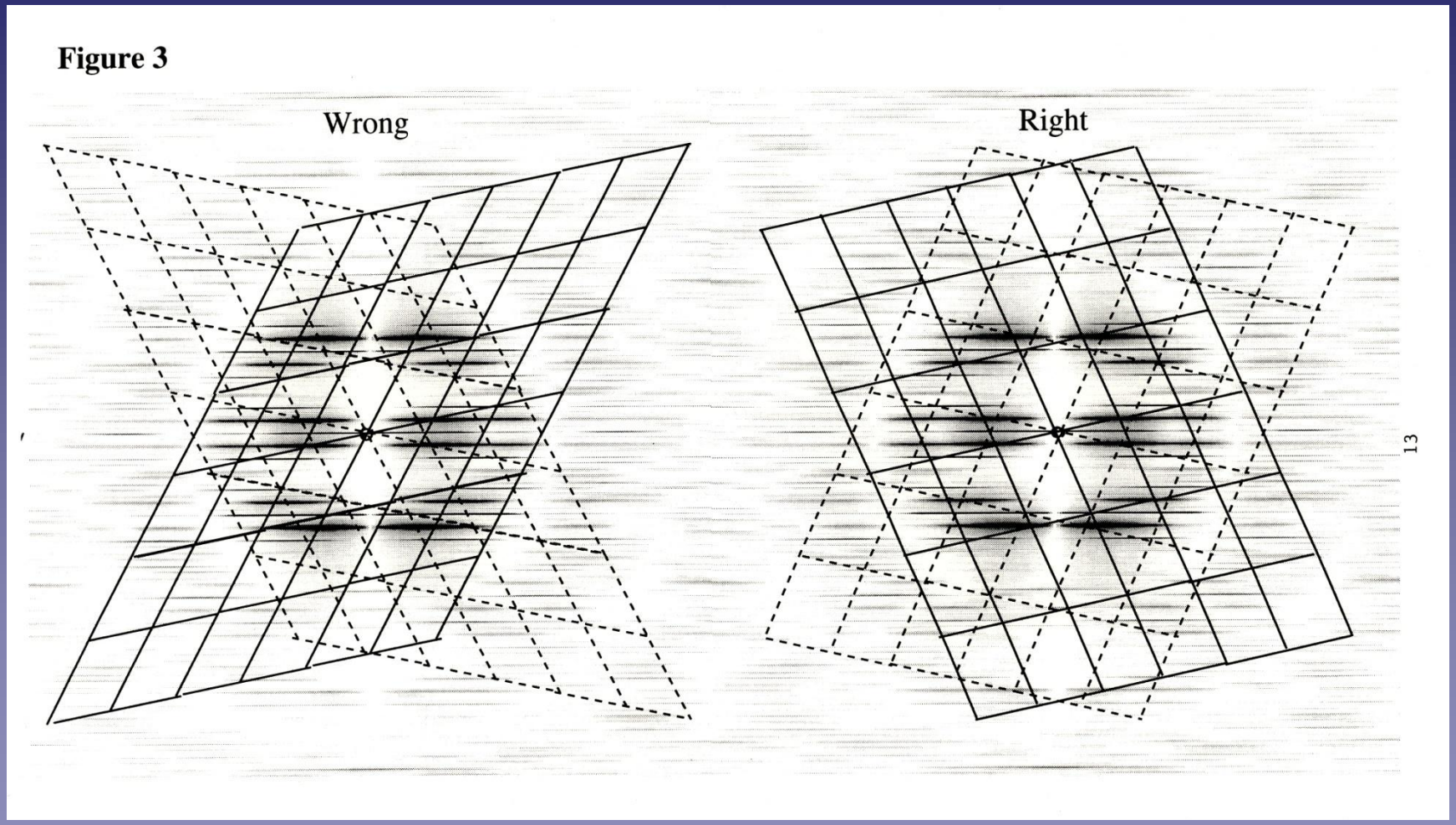

From: How to analyze filaments The principles of helical reconstruction, by David DeRosier
http://www.biomachina.org/courses/structures/download/derosier_handout_02.pdf

Determining the hand of the helical path by EM metal shadowing

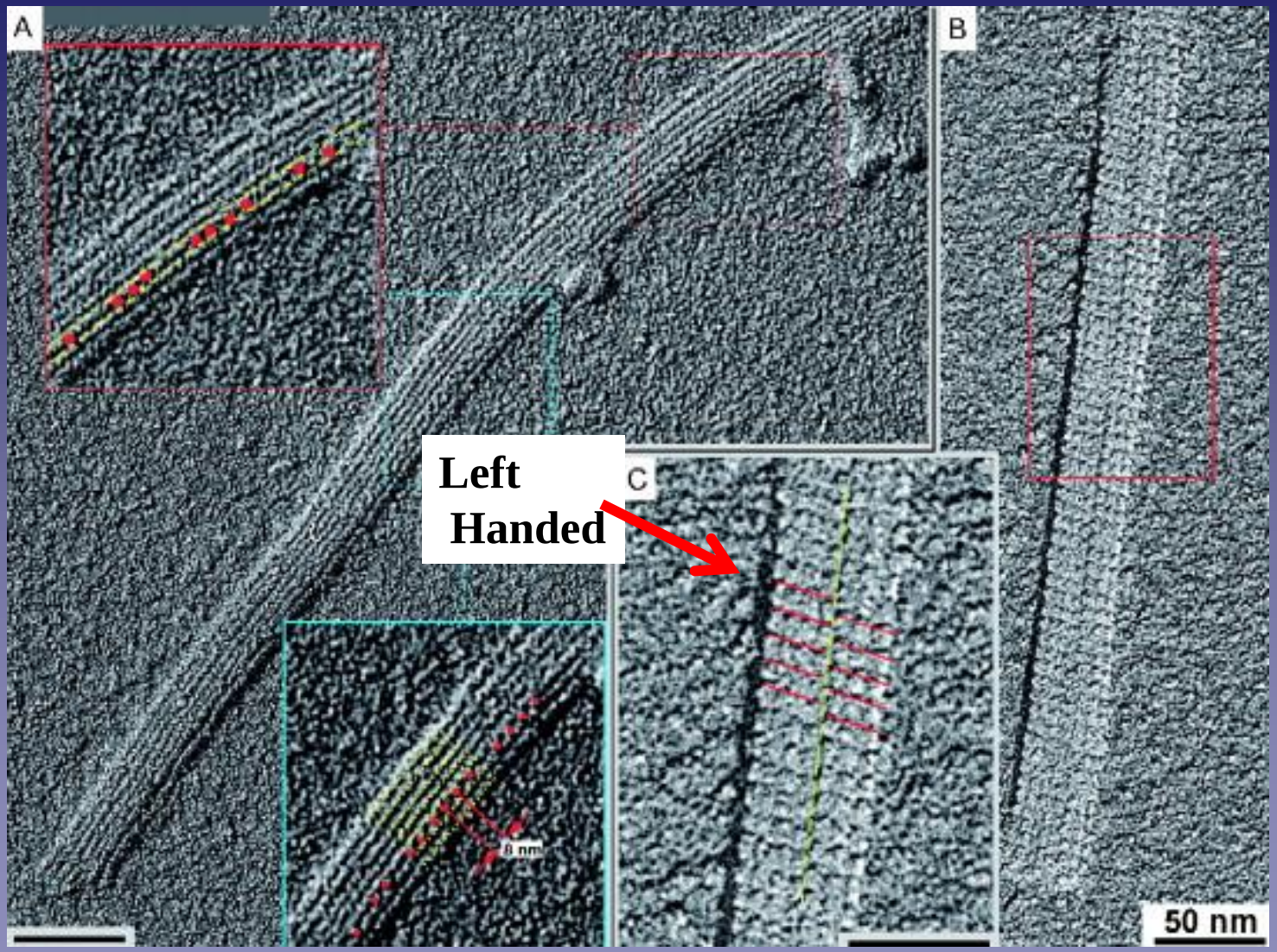

From: Hoenger & Gross J.Struct.Biol. 84: 425 (2008)

Determining the hand of the helical path by tilting specimen

Left handed

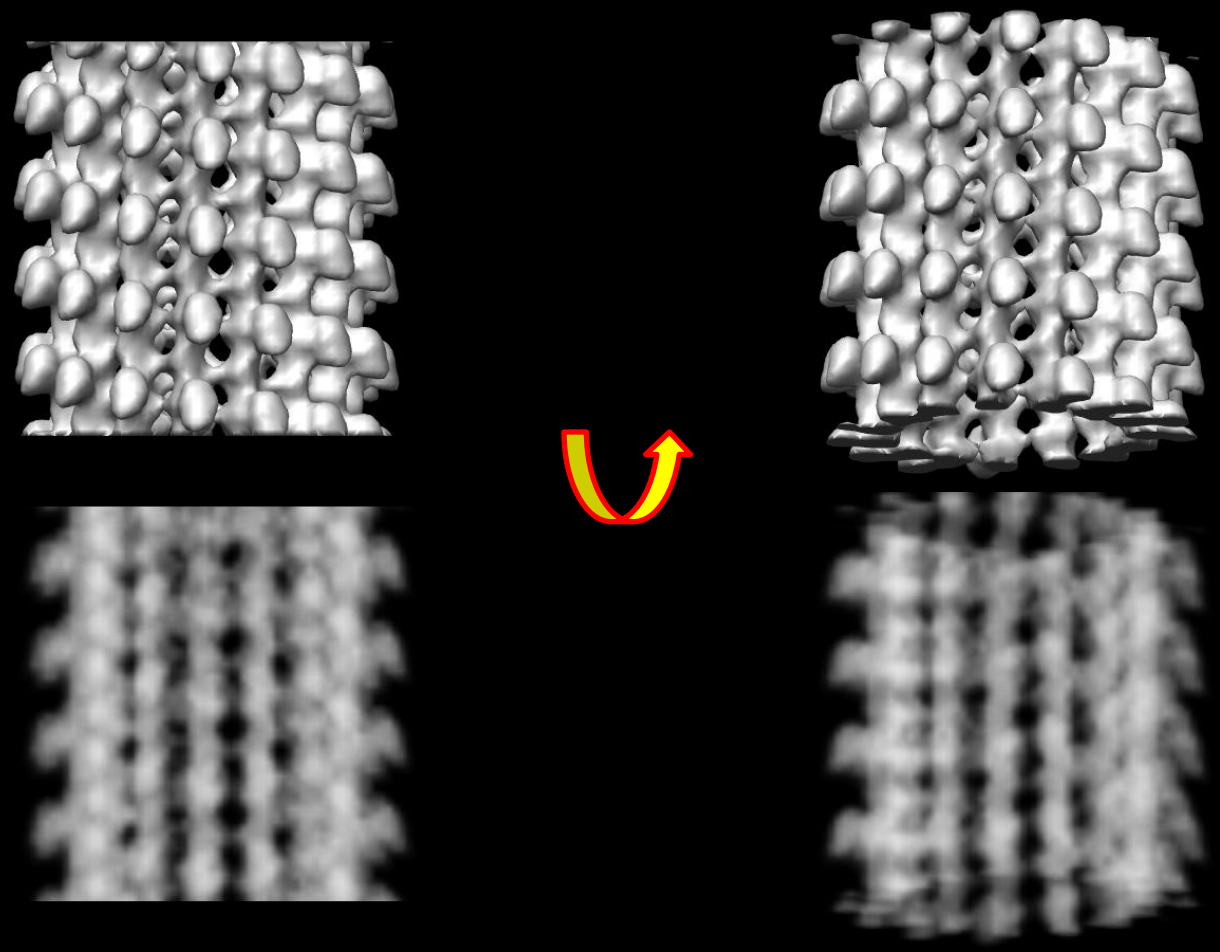

Serrated Pattern on Left

Left Handed

Helical 3D reconstruction Using the Fourier-Bessel Method

DeRosier & Moore J. Mol. Biol. 52:335 1970

358 D. J. DeROSIER AND P. B. MOORE

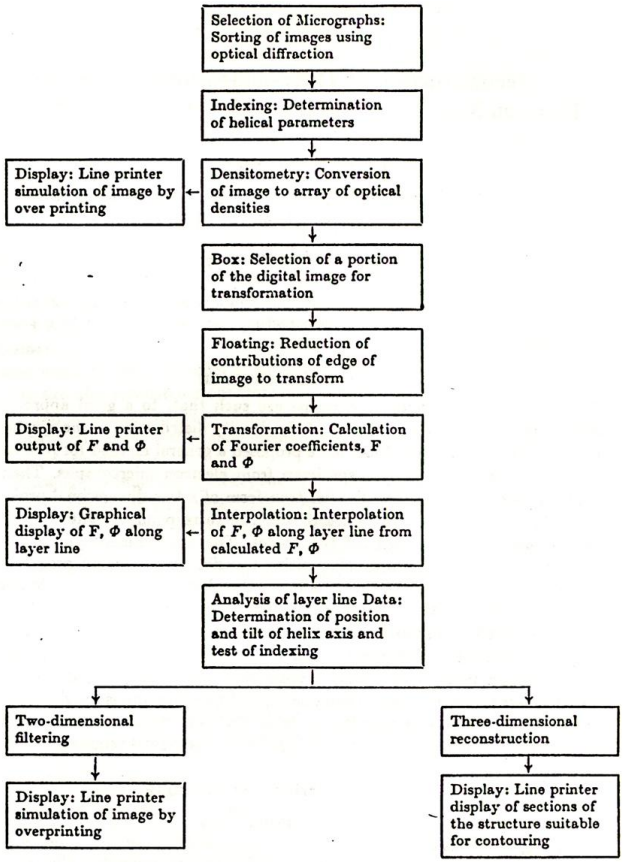

FIG. 1. The scheme presented shows the flow of data in the process of three-dimensional reconstruction.

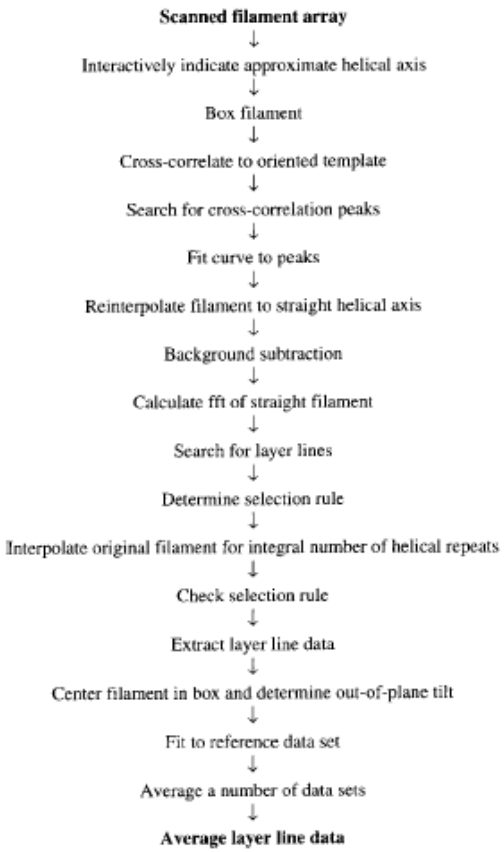

FIG. 1. Schematic diagram of the PHOELIX helical processing package. A detailed description of each step and the programs used is available as part of the PHOELIX distribution.

Helical 3D reconstruction Using the Fourier-Bessel Method

DeRosier & Moore J. Mol. Biol. 52:335 1970

Fourier Transform
Reciprocal Space Function

$$F(R, \Phi, l/c) = \sum_n G_{n,l}(R) \exp\left[in\left(\Phi + \pi/2\right)\right]. \quad (1)$$

Selection rule

$$l = tn + um \quad (2)$$

Real space function
(structure)

$$\rho(r, \phi, z) = \sum_l \sum_n g_{n,l}(r) \exp(in\,\phi) \exp\left(-2\pi i l z/c\right) \quad (3)$$

$$g_{n,l}(r) = \int G_{n,l}(R) J_n(2\pi R r)\, 2\pi R \mathrm{d}R$$

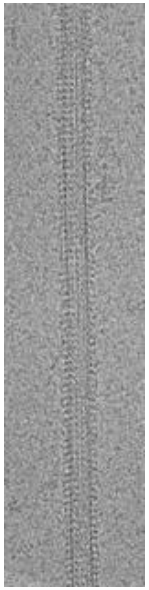

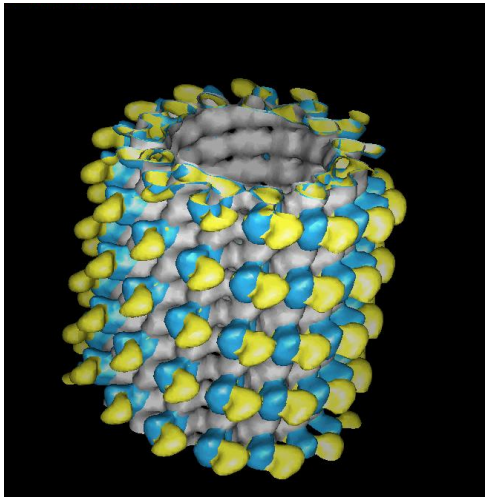

Boxing & Floating Image

Image

FFT

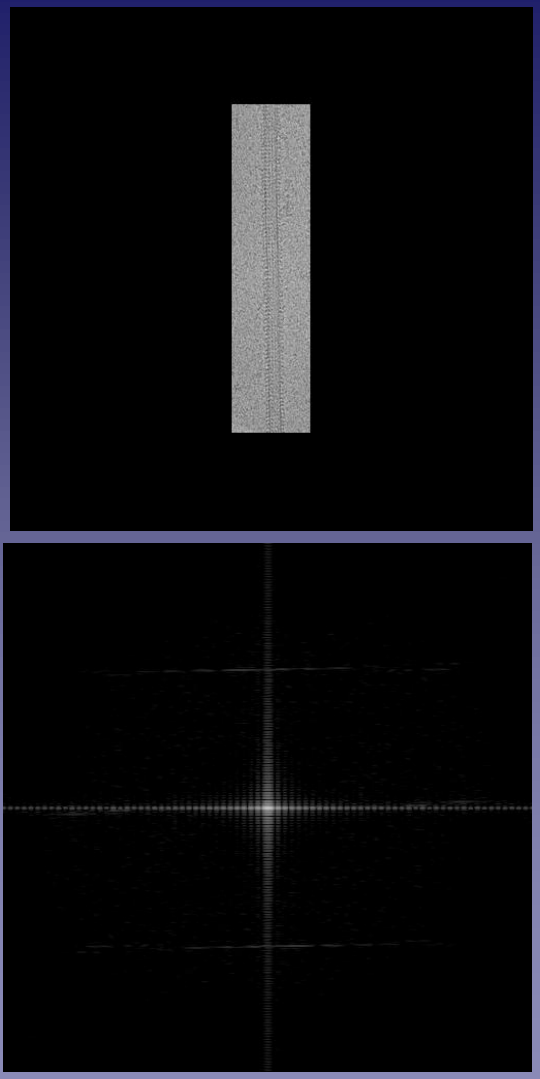

Non-Floated

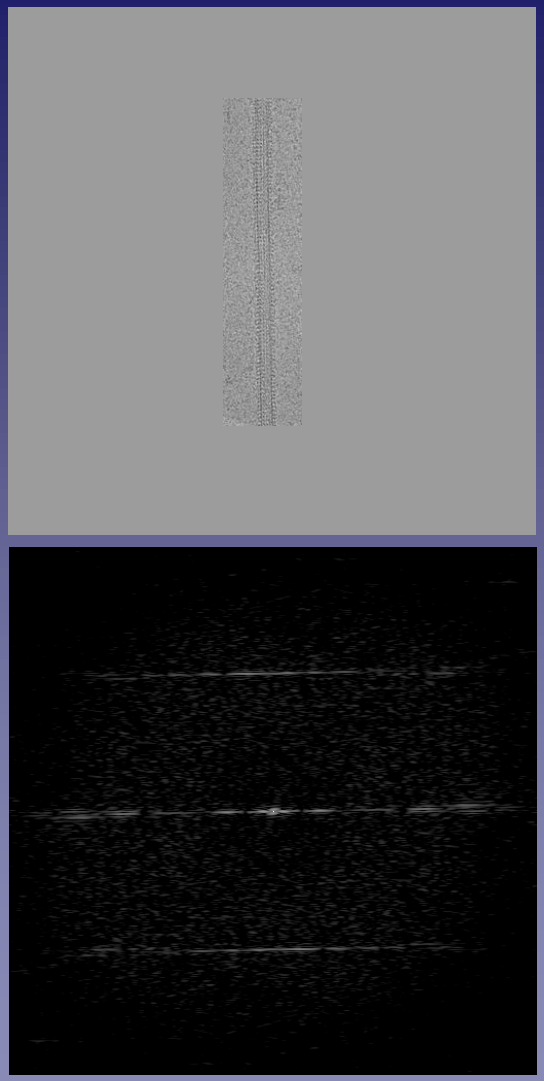

Floated

Straightening

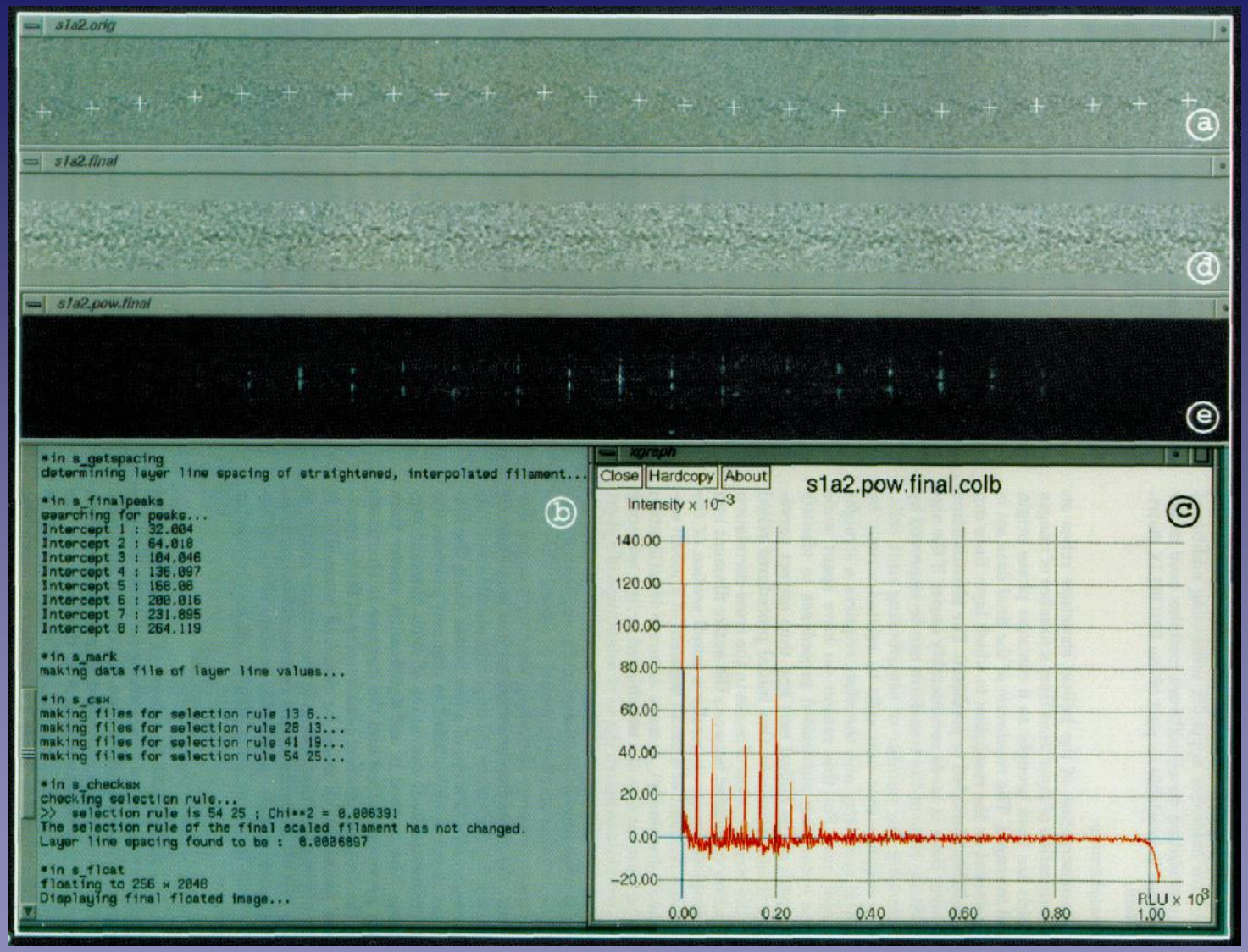

From: Carragher et al., JSB 116: 107-112 (1996)

Gathering Amplitude and Phases

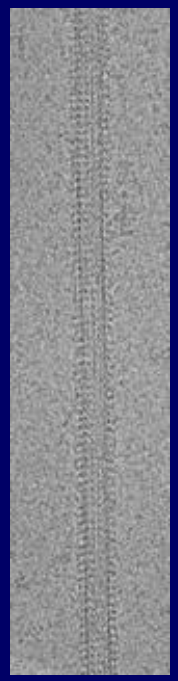

Image

FFT

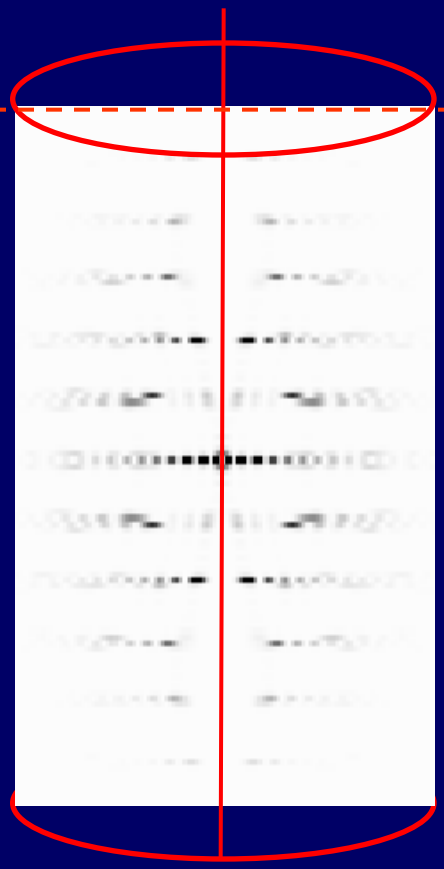

Fourier Transform

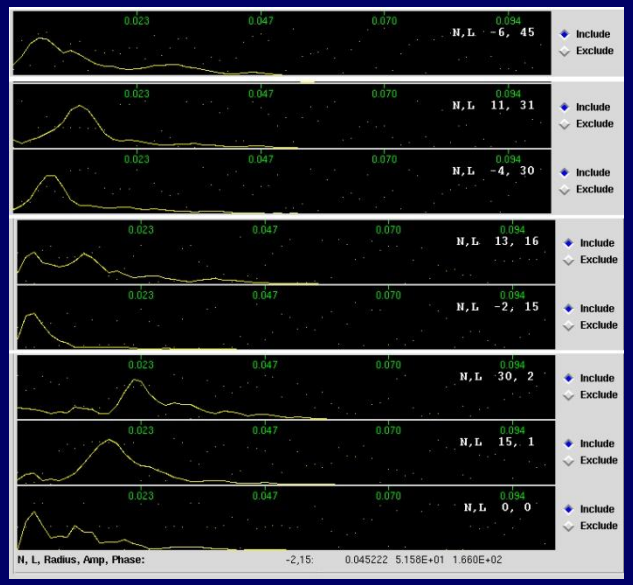

Layer Line Data Set

$$F(R,\psi,l/c) = \sum_n G_{n,l}(R)\exp\left[in(\psi+\tfrac{1}{2}\pi)\right],$$

$$F(R,-\pi/2,l/c) = G_{n,l}$$

$$F(R,+\pi/2,l/c) = \begin{cases} G_{n,l} & \text{(for even n)} \\ -G_{n,l} & \text{(for odd n)} \end{cases}$$

Filament image corrections

Plane Shift and out of plane tilt corrections

Phases Differences in Mirror symmetric peaks from the meridian are predicted. 180^0 for odd n & 0 for even n.

Plane shift and out of plane tilt produce systematic phase differences that can be corrected.

$$F(R, \Phi, l/c) = \sum_n G_{n,l}(R) \exp\left[in\left(\Phi + \pi/2\right)\right].$$

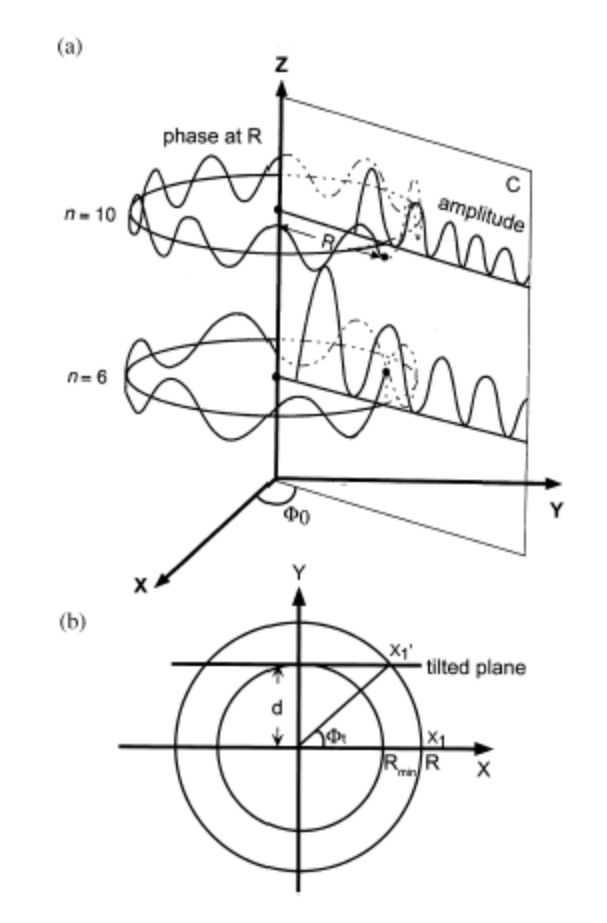

$$\Delta\alpha_{tilt} = -2n \times \tan^{-1}\left(\frac{Z\sin(\omega)}{R}\right).$$

$$\Delta\alpha_{shift} = 4\pi R \Delta x.$$

Lattice distortion Corrections

Alignemt of short filament segments (1/3 of local repeat length) against a reference structure

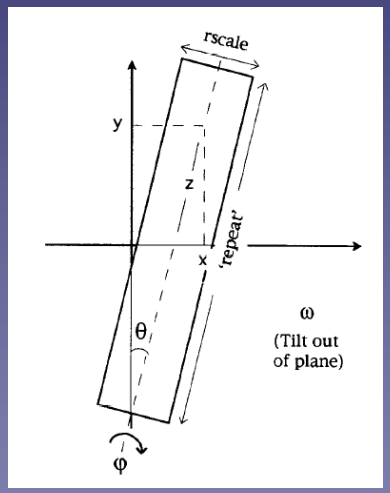

stretch, bend, helical twist, flattening, tilt, shrinkage.

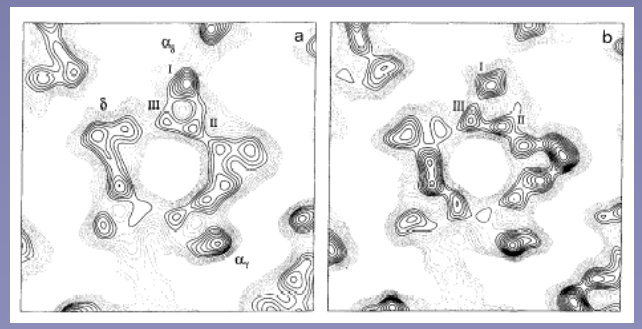

Uncorrected Corrected

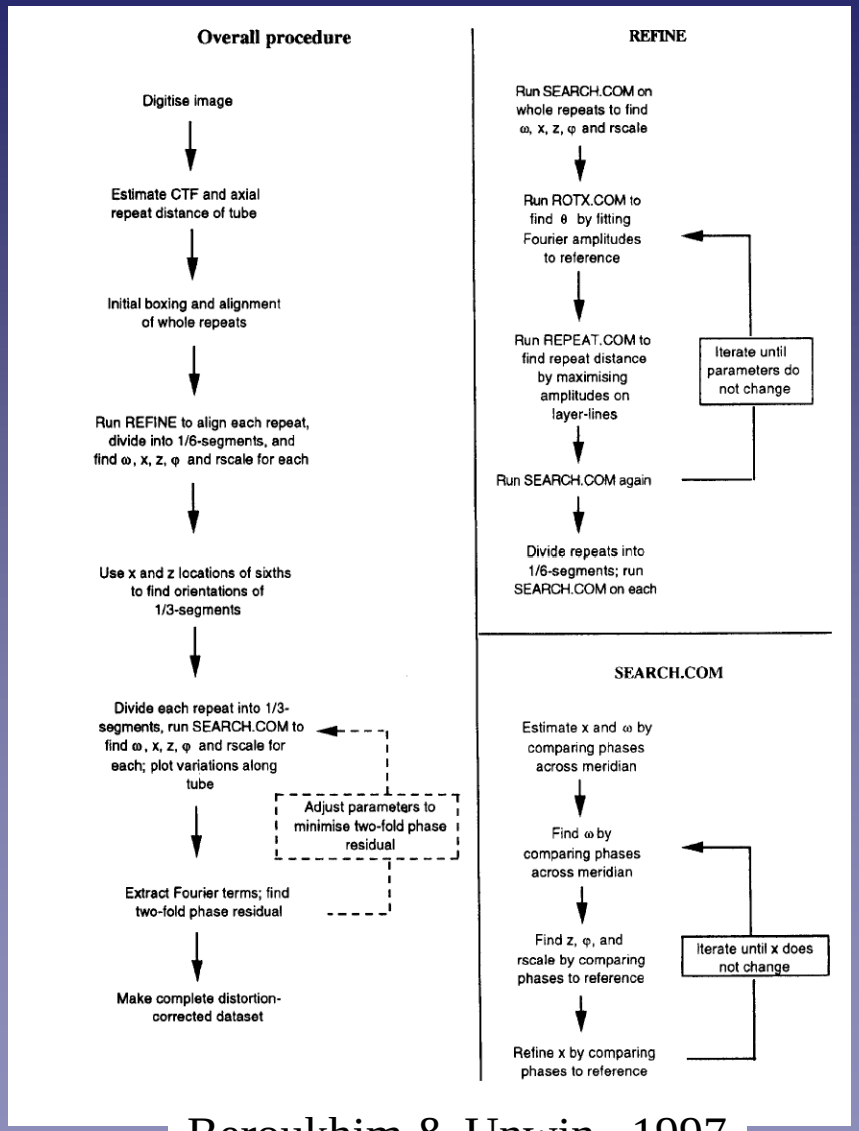

Beroukhim & Unwin. 1997

Averaging several filament/images:

Case 1: Identical helical symmetry (selection rule).

Case2: Slightly different symmetry.

Case 3: Different Helical classes

Case 1: Same symmetry (same selection rule)

1) Rotate and Z displace filaments to the same origin. (Minimize phase differences in layer line data sets)

$$G'_{n,Z}(R, Z) = G_{n,Z}(R, Z)\, e^{-in\Delta\phi + 2\pi i \Delta z Z}$$

ΔΦ: Azimuthal angle difference
Δz: Shift along the axis

$$\sqrt{\langle \Delta\alpha_W^2 \rangle} = \sqrt{\frac{1}{\sum_n \sum_j |G_{n,Z}(R_j, Z_n)|} \sum_n \sum_j |G_{n,Z}(R_j, Z_n)|\, |\alpha(R_j, Z_n) - \overline{\alpha}(R_j, Z_n)|^2}$$

Phase residual

2) Average layer line data sets (CTF weighted average if necessary)

Case 2: Slightly different symmetry due to slight winding or unwinding of the helix resulting in changes in axial repeat distance.

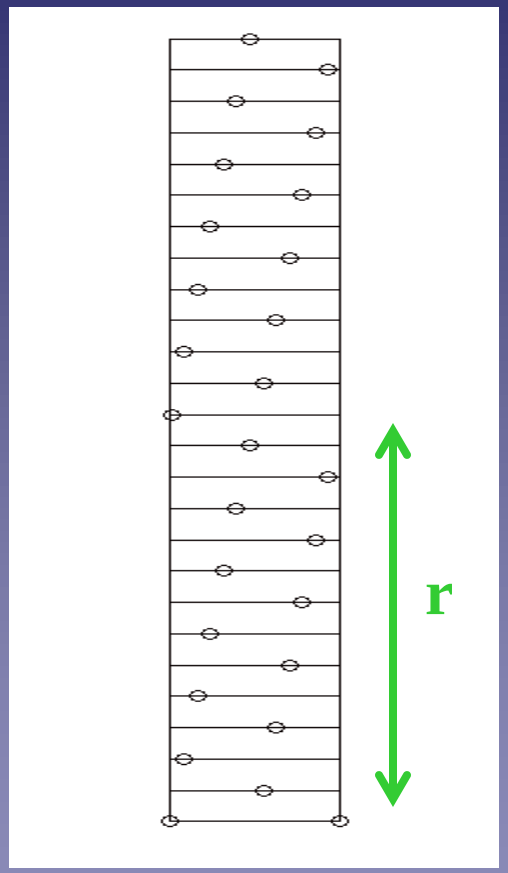

13 units in 6 Turns (LH)

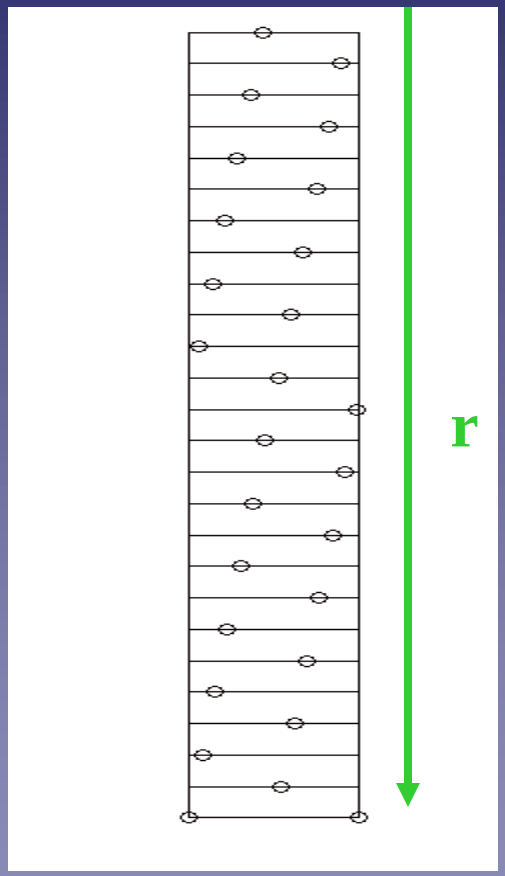

54 units in 25 Turns (LH)

Very similar spacings & bessel orders (n) but different layer line number (l).

l	***n***(|*n*|<7)
0	0
1	2
2	4
3	6
4	-5
5	-3
6	-1
7	1
8	3
9	5
10	-6
11	-4,
12	-2
13	0

13 units in 6 Turns (LH)

l	***n***(|*n*|<7)
0	0
4	2
8	4
12	6
17	-5
21	-3
25	-1
29	1
33	3
37	5
42	-6
46	-4
50	-2
54	0

54 units in 25 Turns (LH)

Case 3: Different Helical Classes

Method 1, Fourier Space Method:

Apply appropiate phase and radial shift to $g_{ni}(r,Z)$ values from different particles and then average them.

Use: If all particles have identical 2D lattices but different circumferential vectors.

DeRosier, Stokes & Darst. J. Mol. Biol. 289: 159 (1999)

$$F(R, \Phi, l/c) = \sum_n G_{n,l}(R) \exp\left[in\left(\Phi + \pi/2\right)\right].$$

$$g_{n,l}(r) = \int G_{n,l}(R) J_n(2\pi Rr)\, 2\pi R \mathrm{d}R$$

$$\rho(r, \phi, z) = \sum_l \sum_n g_{n,l}(r) \exp(in\,\phi) \exp\left(-2\pi i l z/c\right)$$

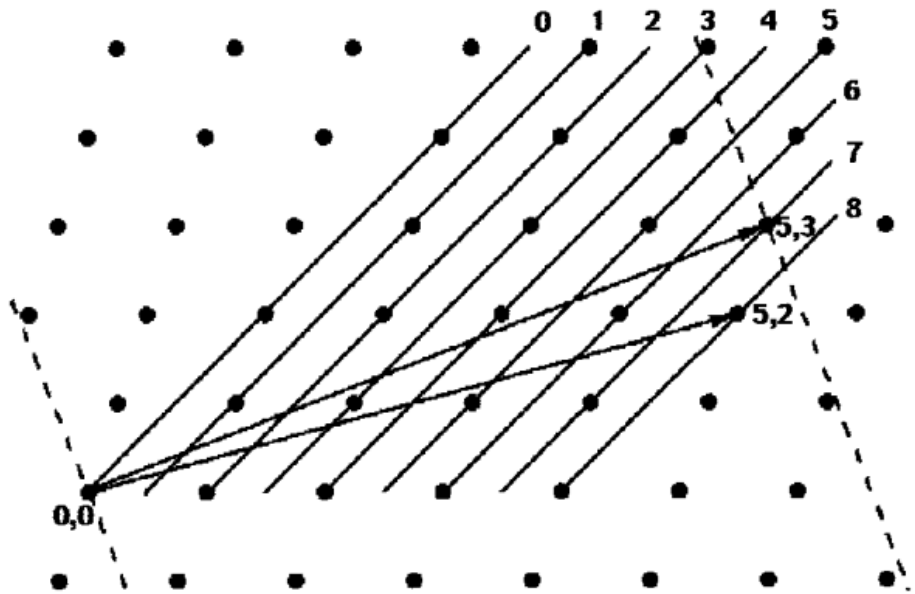

Case 3: Different Helical Classes

Method 2, Real Space Method:

- Calculate separate 3D reconstructions for each filament.

- Carve out the asymmetric unit on each of the reconstructions.

- Generate a new artificial layer line set for each reconstruction by applying helical symmetry (the same for all particles) to the carved out asymmetric unit.

- Align the artificial helices in reciprocal space and average their layer line data (as normally done in Fourier-Bessel helical reconstruction).

- Obtain an averaged map by Fourier Bessel inversion.

Zhang et al., Nature 392: 835-840 (1998).
Yonekura & Toyoshima. Ultramicroscopy 84: 15-28 (2000)

Is it always a single view enough for helical 3D reconstruction ?

Yes: If there is no overlap of Bessel functions at the resolution of interest. No if there is overlap.

l	***n***(*|n|<=10*)
0	0
1	2
2	4, -9
3	6
4	-5, 8
5	-3, 10
6	-1
7	1
8	3, -10
9	5, -8
10	-6, 7
11	-4, 9
12	-2
13	0

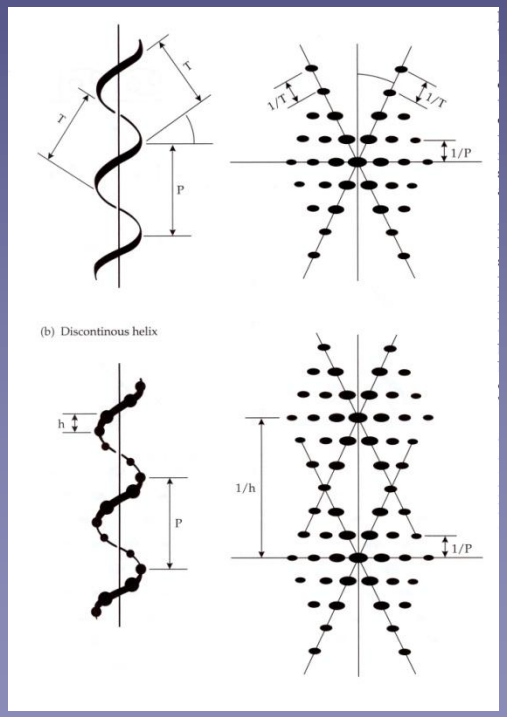

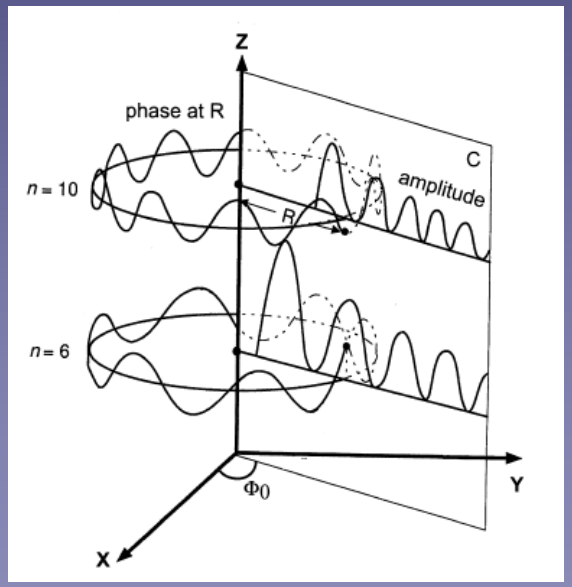

$$l = -6n + 13m$$

Resolution Criteria

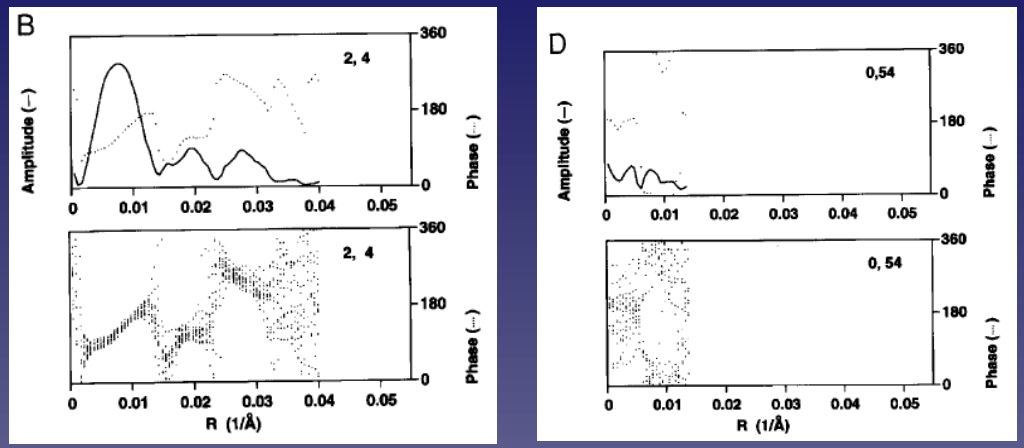

Phase Residuals Along layer lines

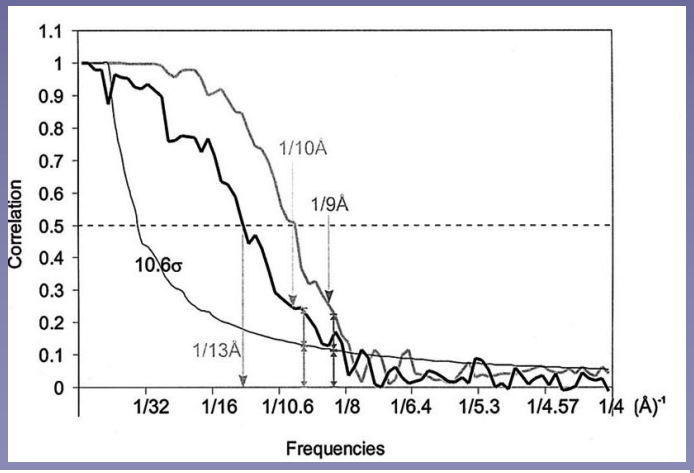

$$\mathrm{FSC}(k,\,\Delta k) = \frac{\sum\limits_{(k,\Delta k)} F_1(\mathbf{k})F_2^{\dagger}(\mathbf{k})}{\left[\sum\limits_{(k,\Delta k)} |F_1(\mathbf{k})|^2 \sum\limits_{(k,\Delta k)} |F_2(\mathbf{k})|^2\right]^{1/2}},$$

Fourier Shell Correlation

Kinesin13-Microtubule Ring Complex Helical Reconstruction

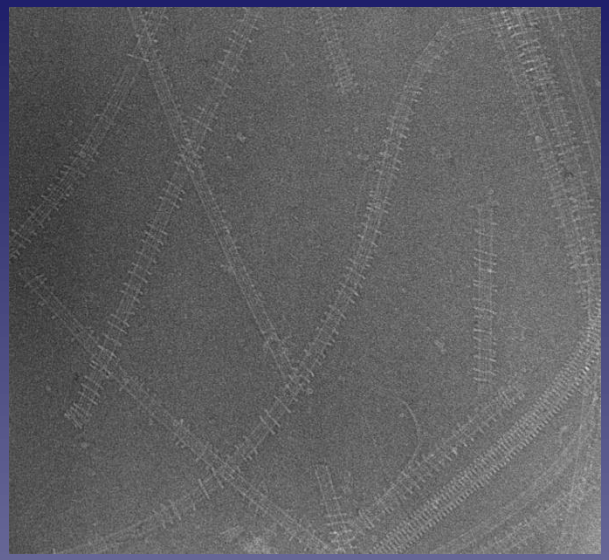

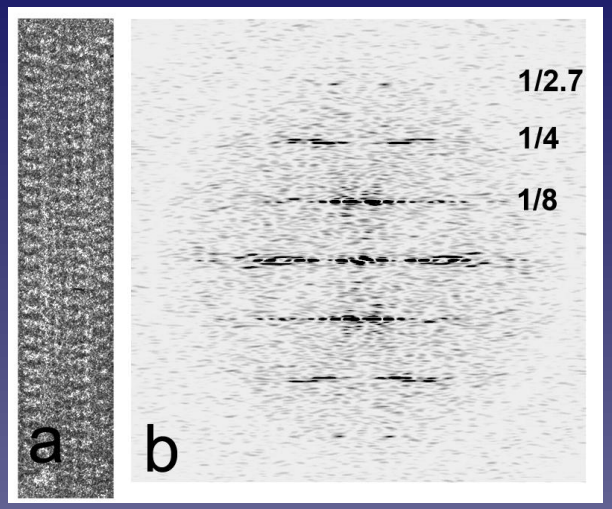

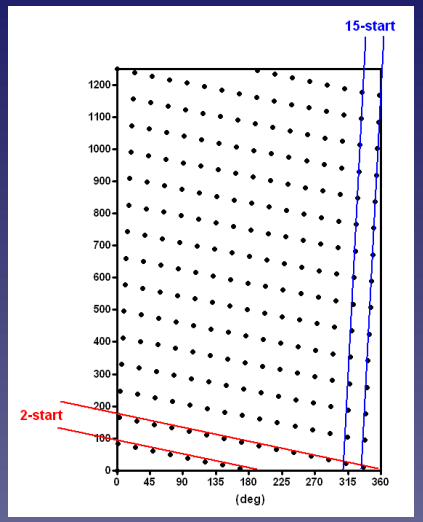

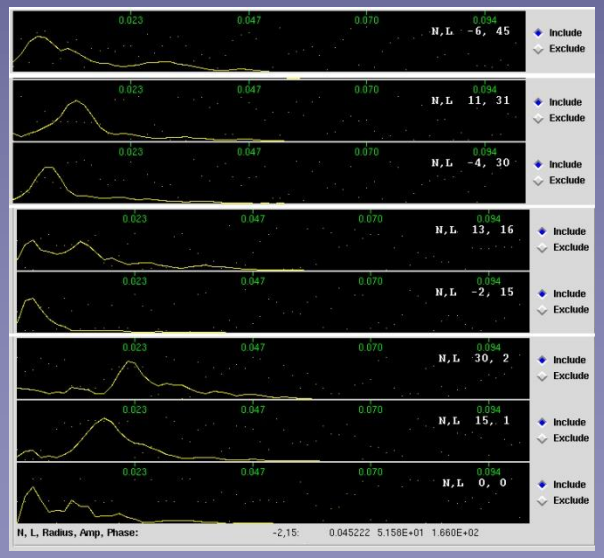

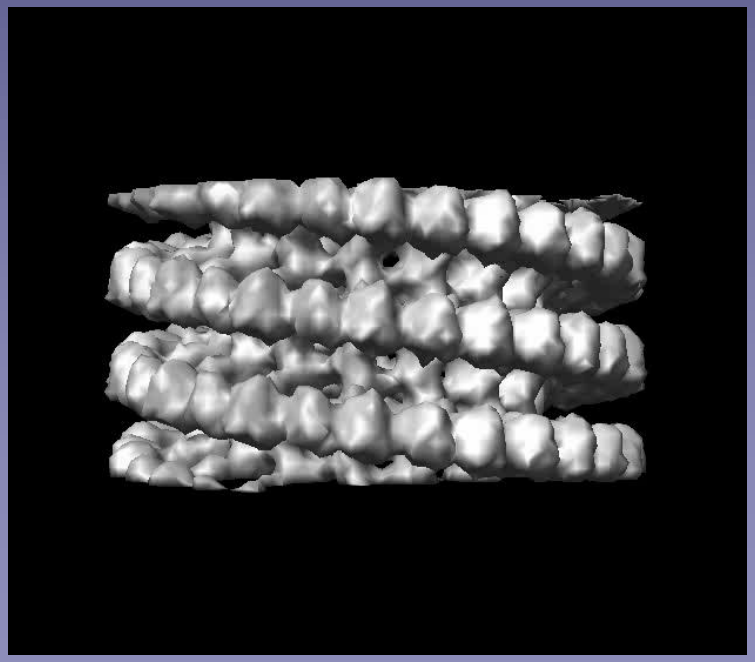

3D Helical Reconstruction Examples (All done by Fourier-Bessel method)

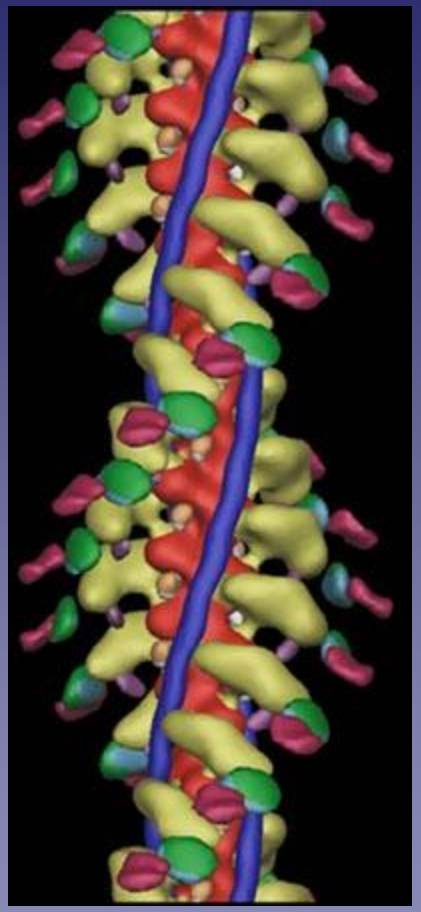

Acto-myosin complex

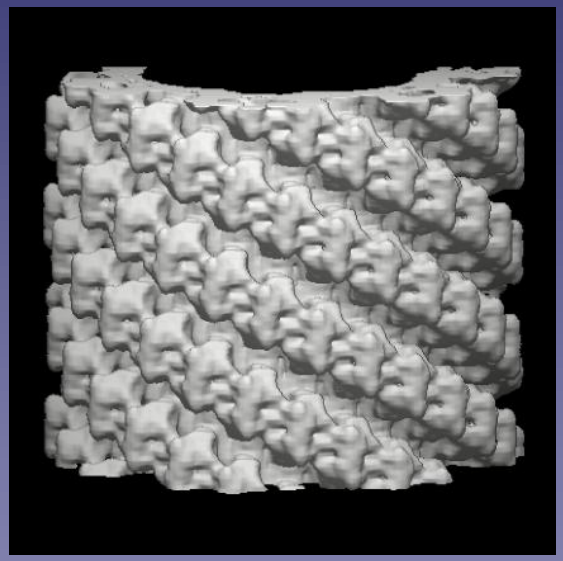

Ca-ATPase
Tubular crystal
E_2 state (VO_4)

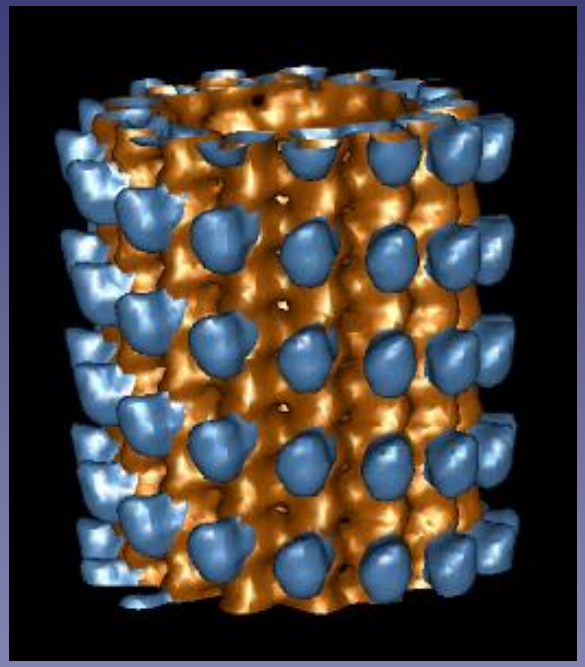

Microtubule-NCD complex

3D Helical Reconstruction Using Real Space Methods

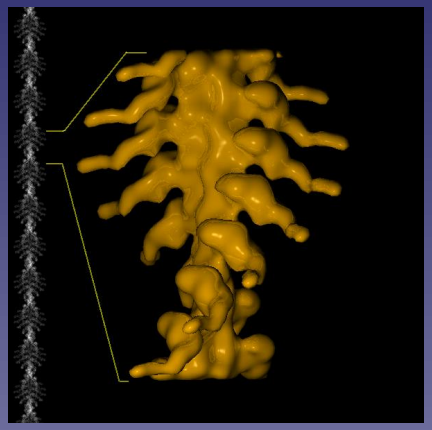

Individual images are boxed out of the filament at each assymetric unit axial spacing and a view angle is assigned according to the helical symmetry of the filament.

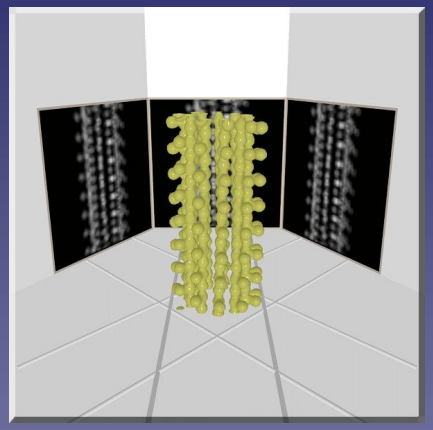

A 3D volumen is obtained by back-projection of the boxed images.

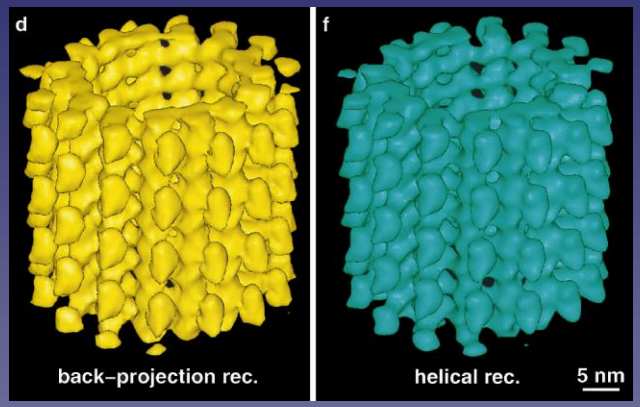

From Sosa et al. JSB 118: 149-158(1997)

3D Helical Reconstruction Using Real Space Methods

A good estimate of the specimen helical symmetry is needed

Axial rise per subunit (h)

Azimuthal angle per subunit (Φ)

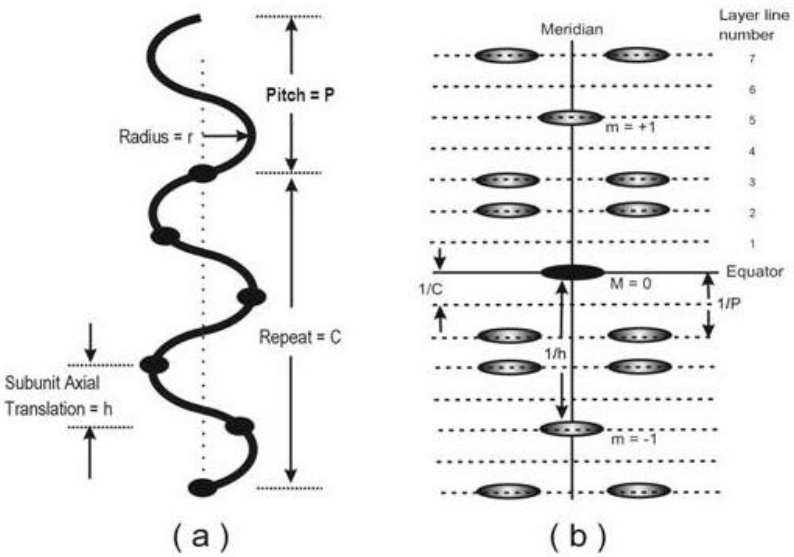

If an appropriate section rule for the specimen is know ($l = tn + um$) h and Ω can be calculated as:

$$h = C / u$$

$$\Phi = t \cdot 360 / u$$

$$C = l / Z$$

***u*:** Num. of subunits per axial repeat.

***t* :** Num. of turns per axial repeat.

***l* :** Layer line number.

C: Helical axial repeat distance.

Z: Layer line height (distance from equator in reciprocal space)

3D Helical Reconstruction Using Real Space Methods and "single particle" refinement

Box Filament segments

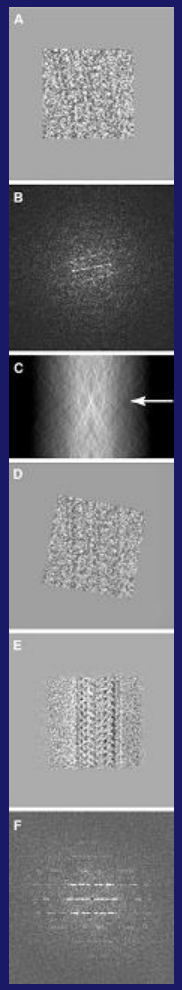

In-plane Rotational Alignment

Multi-reference alignment with atomic models

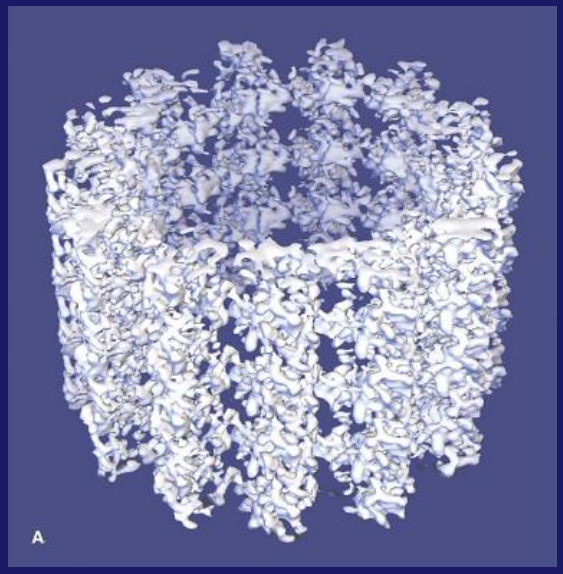

8 Å resolution microtubule map

From: Li et al., (2002) Structure 10: 1317-1328.

The Iterative Helical Real Space Reconstruction Method (IHRSR)

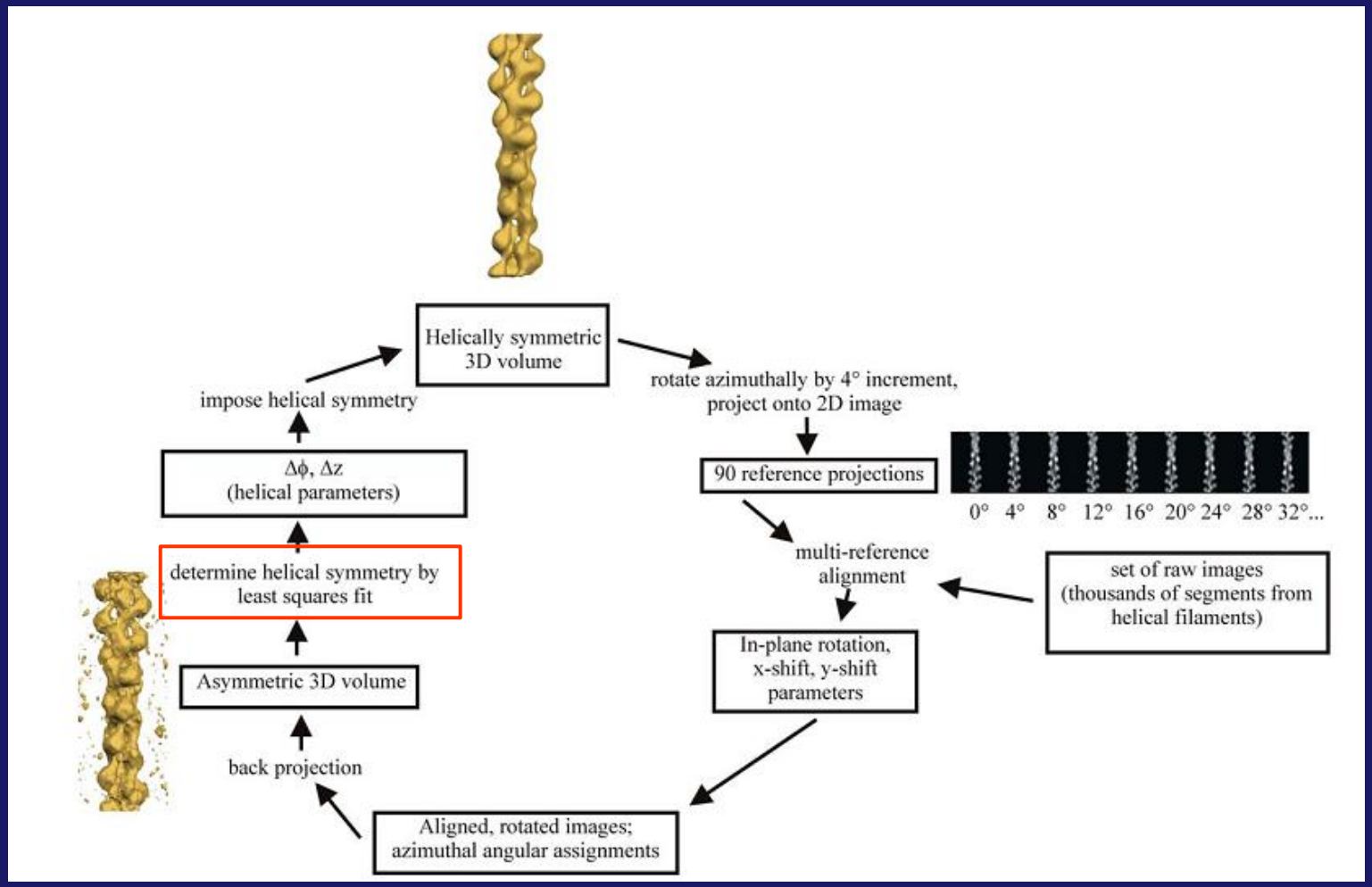

From: Egelman E.H. (2000) Ultramicroscopy 85: 225-234.

Some structures solved using the IHRSR method

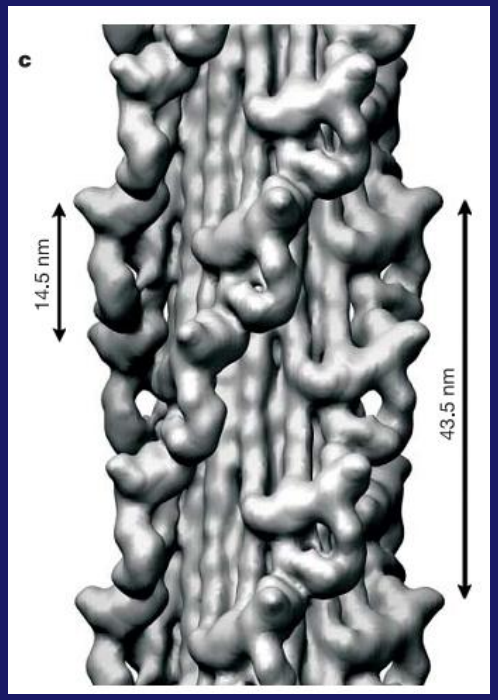

Tarantula striated muscle myosin filament (r=2.5 nm). Woodhead etal., 2005

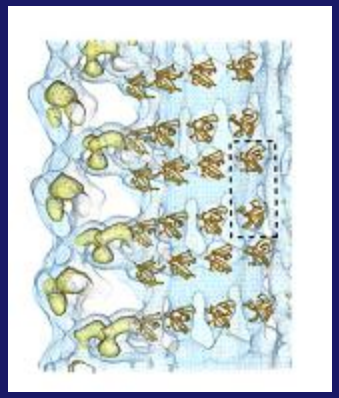

Dynamin (r=0.2nm). (Mears et al., 2007)

Bacteria Adhesion Pili (r=1.25 nm)). Mu et al., (2008)

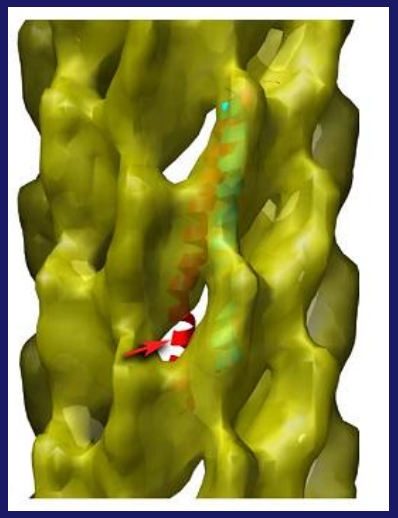

Filamentous Bacteriophage (r=0.8 nm) Wang et al., 2009

Fourier-Bessel method vs. IHRSR:

Pomfret et al., (2007) J. Struct Biol 157: 106

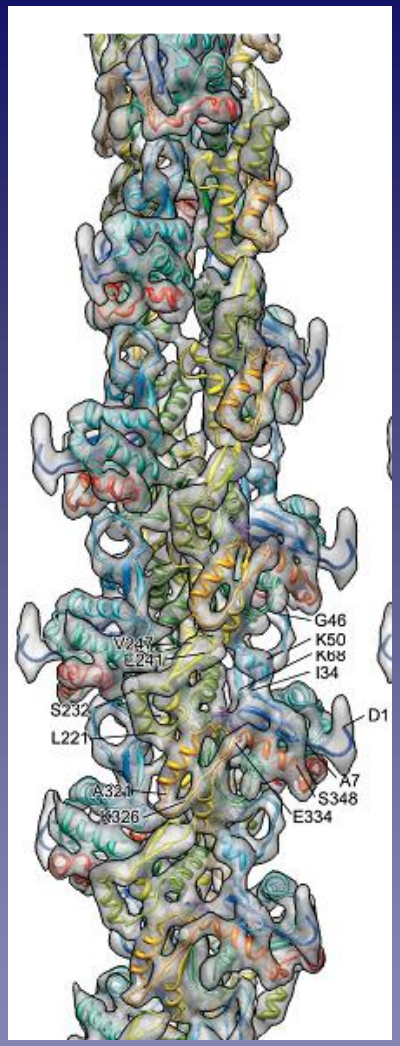

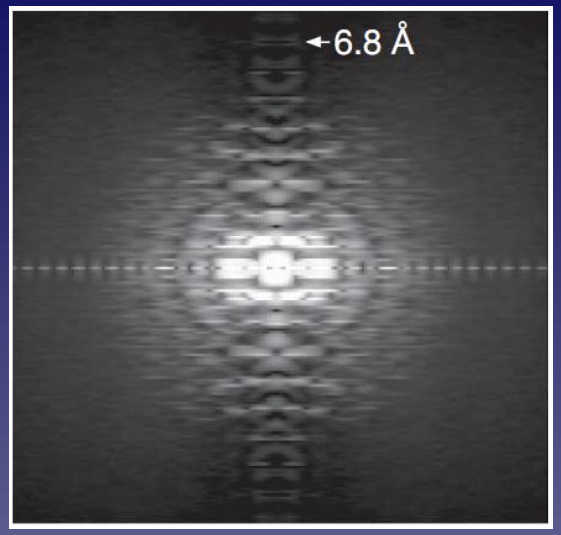

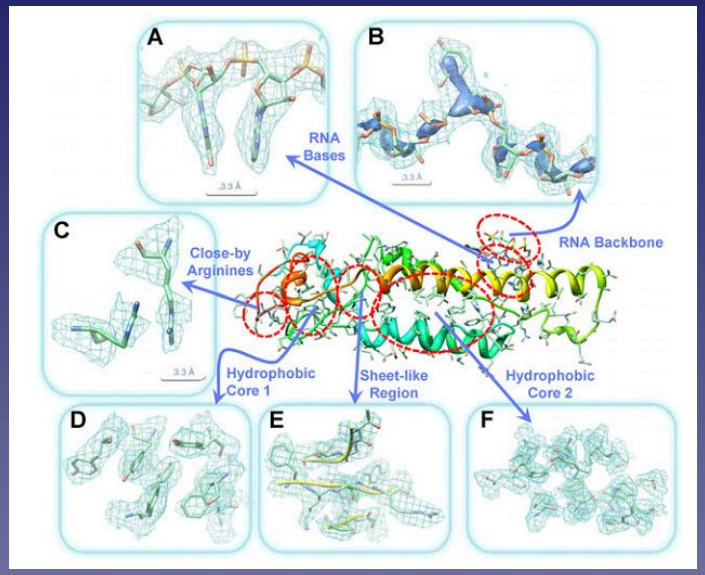

TMV @ 3.3 A Resolution

Ge & Zhou. PNAS 108: 9637 (2011)

(~1.9 x10^6 asymmetric units)

F-Actin @ 6.6 A resolution

Fujii et al. Nature 467: 724 (2010)

(~120000 asymmetric units)

Software for Helical 3D Reconstruction

Fourier-Bessel

- MRC Package
- Brandeis
- Phoelix & Suprim
- Unwin's routines
- Toyoshima's routines
- Ruby-Helix (Kikkawa's lab)
- EMIP (Stoke's lab)

Real space or single–particle-like iterative refinement software

- IHRSR (Egelman's lab)
- SPRING (Sachse' lab)
- FREALIGN (Grigorieff's lab)
- PyHelix (Sosa's lab)
- EMAN, SPARX, SPIDER

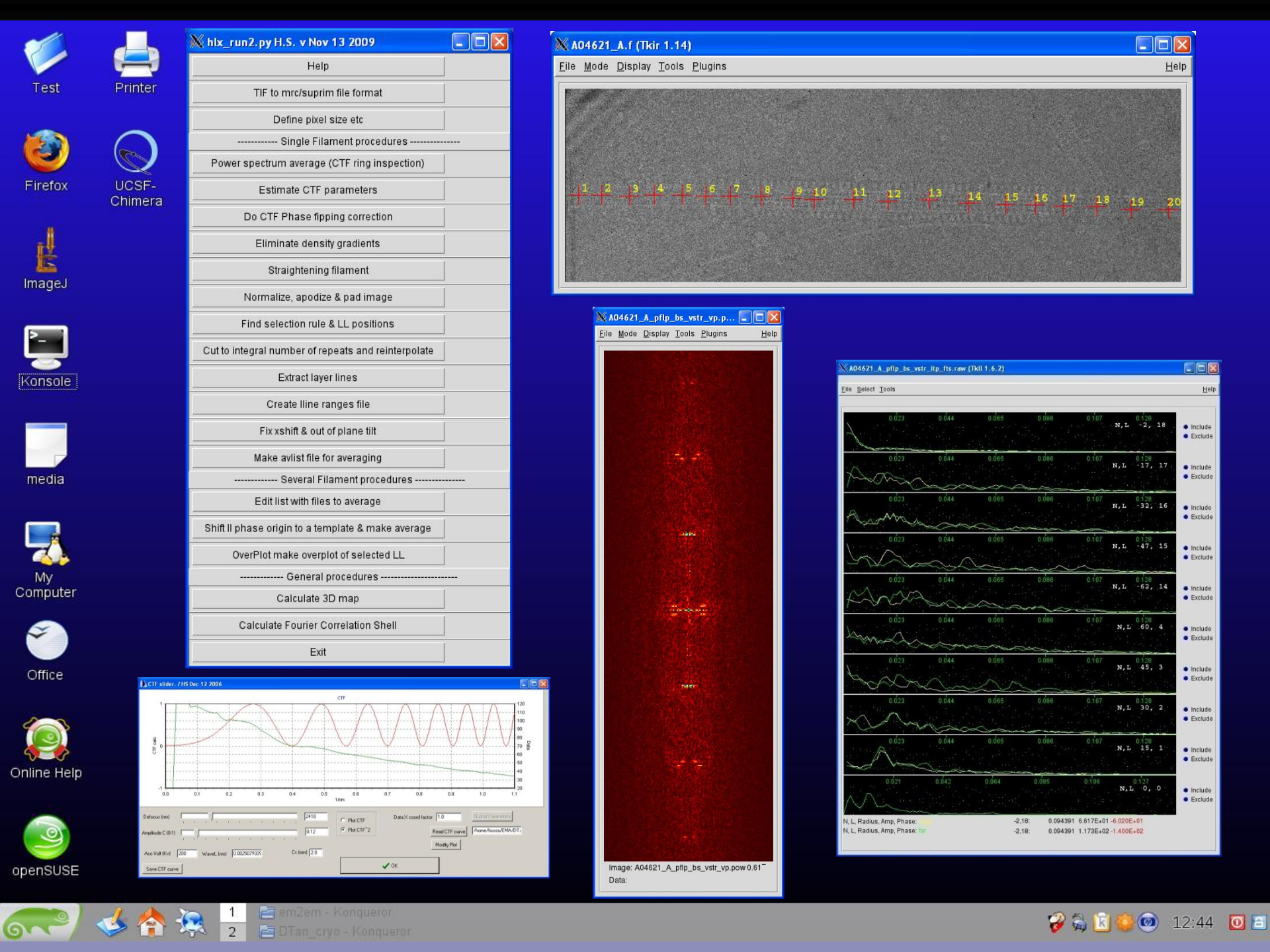
Test
Printer
Firefox
UCSF-Chimera
ImageJ
Konsole
media
My Computer
Office
Online Help
openSUSE
hlx_run2.py H.S. v Nov 13 2009
Help
TIF to mrc/suprim file format
Define pixel size etc
---------- Single Filament procedures ----------
Power spectrum average (CTF ring inspection)
Estimate CTF parameters
Do CTF Phase fipping correction
Eliminate density gradients
Straightening filament
Normalize, apodize & pad image
Find selection rule & LL positions
Cut to integral number of repeats and reinterpolate
Extract layer lines
Create lline ranges file
Fix xshift & out of plane tilt
Make avlist file for averaging
---------- Several Filament procedures ----------
Edit list with files to average
Shift ll phase origin to a template & make average
OverPlot make overplot of selected LL
---------- General procedures ----------
Calculate 3D map
Calculate Fourier Correlation Shell
Exit
A04621_A.f (Tkir 1.14)
File Mode Display Tools Plugins Help
A04621_A_pflp_bs_vstr_vp.p...
Image: A04621_A_pflp_bs_vstr_vp.pow 0.61
Data:
A04621_A_pflp_bs_vstr_itp_fts.raw (Tkll 1.6.2)
File Select Tools Help
Include
Exclude
CTF slider. / HS Dec 12 2006
em2em - Konqueror
DTan_cryo - Konqueror
12:44

Atomic Modeling & Docking of Higher Resolution Structures into EM maps

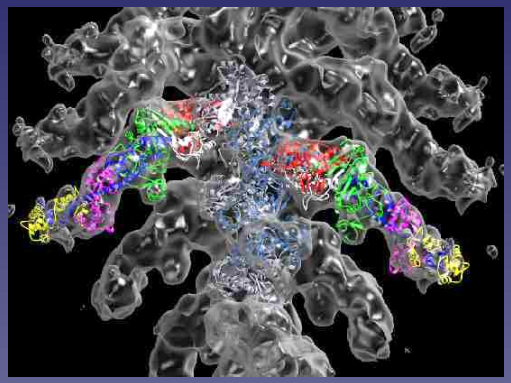

Acto-myosin complex

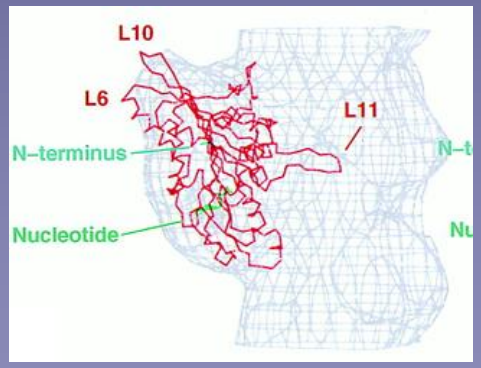

Microtubule-NCD complex

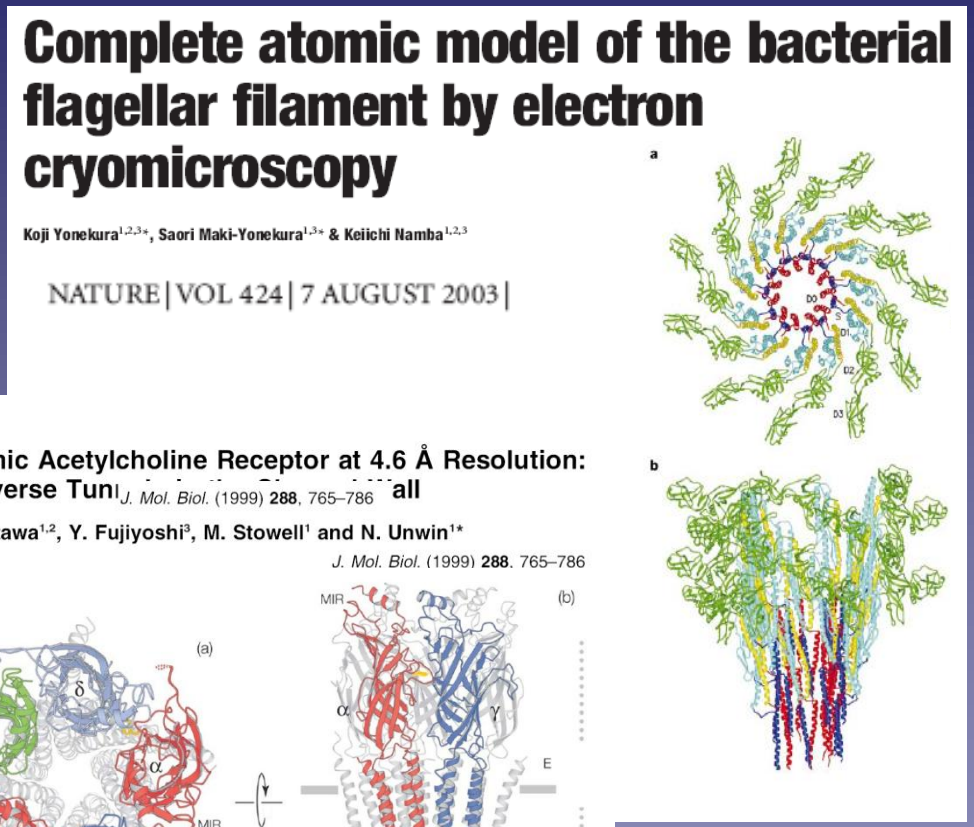

Complete atomic model of the bacterial flagellar filament by electron cryomicroscopy

Koji Yonekura[1,2,3]*, Saori Maki-Yonekura[1,3]* & Keiichi Namba[1,2,3]

NATURE | VOL 424 | 7 AUGUST 2003 |

Nicotinic Acetylcholine Receptor at 4.6 Å Resolution: Transverse Tunnels in the Channel Wall

A. Miyazawa[1,2], Y. Fujiyoshi[3], M. Stowell[1] and N. Unwin[1]*

J. Mol. Biol. (1999) **288**, 765–786

Bibliography

Fourier–Bessel Reconstruction of Helical Assemblies. Diaz, R. Rice W. J. and Stokes D.L. Methods in Enzymology. (2010) **482**: 131-165. 2010

Electron Crystallography of Helical Structures. Chapter 12 in Electron Crystallography of Biological Macromolecules (2007). Glaeser R.M., Downing K., DeRosier D., Chiu W. and Frank J. Oxfrod University Press

Cochran, W., F.H.C. Crick, and V. Vand. 1952. The Structure of Synthetic Polypeptides. I. The Transform of Atoms on a Helix. *Acta Crystallographica*. 5:581-586.

Klug, A., F.H.C. Crick, and H.W. Wyckoff. 1958. Diffraction by Helical Structures. *Acta Crystallographica*. 11:199-213.

DeRosier, D.J., and P.B. Moore. 1970. Reconstruction of three-dimensional images from electron micrographs of structures with helical symmetry; *J Mol Biol*. 52:355-69.

Egelman, E.H. 1986. An algorithm for straightening images of curved filamentous structures. *Ultramicroscopy*. 19:367-73.

Stewart, M. 1988. Computer image processing of electron micrographs of biological structures with helical symmetry. *J Electron Microsc Tech*. 9:325-58.

Sosa, H., and R.A. Milligan. 1996. Three-dimensional structure of ncd-decorated microtubules obtained by a back-projection method. *J Mol Biol*. 260:743-55.

Young, H.S., J.L. Rigaud, J.J. Lacapere, L.G. Reddy, and D.L. Stokes. 1997. How to make tubular crystals by reconstitution of detergent-solubilized Ca2(+)-ATPase. *Biophys J*. 72:2545-58.

DeRosier, D., D.L. Stokes, and S.A. Darst. 1999. Averaging data derived from images of helical structures with different symmetries. *J Mol Biol*. 289:159-65.

Egelman, E.H. 2000. A robust algorithm for the reconstruction of helical filaments using single-particle methods. *Ultramicroscopy*. 85:225-34.

Toyoshima, C. 2000. Structure determination of tubular crystals of membrane proteins. I. Indexing of diffraction patterns. *Ultramicroscopy*. 84:1-14.

Yonekura, K., and C. Toyoshima. 2000. Structure determination of tubular crystals of membrane proteins. II. Averaging of tubular crystals of different helical classes. *Ultramicroscopy*. 84:15-28.